Pre-Conceptual Design Report (pCDR)
for
The Science and Experimental Equipment
for
The 12 GeV Upgrade of CEBAF

Draft 12.1

Jefferson Lab

June 10, 2003

Jefferson Lab is managed and operated by
the Southeastern Universities Research Association (SURA) for
the Office of Science of the U.S. Department of Energy.

Thomas Jefferson National Accelerator Facility
12000 Jefferson Avenue
Newport News, VA 23606
www.JLab.org
(757)-269-7100

Abstract

This Pre-Conceptual Design Report (pCDR) presents the compelling scientific case for upgrading the Continuous Electron Beam Accelerator Facility (CEBAF) at Jefferson Lab to 12 GeV. Such a facility will make profound contributions to the study of nuclear matter. In particular, it will allow breakthrough programs to be launched in four main areas:

- *The experimental study of gluonic excitations in order to understand the fundamentally new dynamics that underpins all of nuclear physics: the confinement of quarks.* Theoretical conjectures, now strengthened by lattice QCD simulations, indicate that the most spectacular new prediction of QCD – quark confinement – occurs through the formation of a string-like "flux tube" between quarks. This conclusion (and proposed mechanisms of flux tube formation) can be tested by determining the spectrum of the gluonic excitations of mesons.

- *The determination of the quark and gluon wavefunctions of the nuclear building blocks.* A vast improvement in our knowledge of the fundamental structure of the proton and neutron can be achieved. Not only can existing "deep inelastic scattering" cross sections be extended for the first time to cover the critical region where their basic three-quark structure dominates, but also measurements of new "deep exclusive scattering" cross sections will open the door to a comprehensive characterization of these wavefunctions using the framework of the Generalized Parton Distributions; these data will provide direct access to information on the correlations among the quarks. These studies will be complemented by detailed measurements of elastic and transition form factors, determining the dynamics underlying the quark-gluon wavefunctions through measurements of their high-momentum-transfer behavior and providing essential constraints on the wavefunctions.

- *Exploring the limits of our understanding of atomic nuclei.* A broad and diversified program of measurements that (taken together with the hadron studies outlined above) aims to provide a firm intellectual underpinning for all of nuclear physics by answering the question "How does the phenomenological description of nuclei as nucleons interacting via an effective interaction parameterized using meson exchange arise from the underlying dynamics of quarks and gluons?" It has two main components:

  The short-range behavior of the Nucleon–Nucleon ($N-N$) interaction and its QCD basis. Experiments aimed at identifying the physics of strong QCD that gives rise to the $N-N$ force and exploring the short range behavior of the $N-N$ force through a novel program of deep inelastic scattering.

  Identifying and exploring the transition from the nucleon/meson description of nuclei to the underlying quark and gluon description. This program will explore and determine the limits of applicability of the nucleon/meson description of nuclei, identifying the distance and energy scales at which it fails and the physics of nuclei is better described directly via strong QCD.

- *Tests of the Standard Model of electro-weak interactions and the determination of fundamental parameters of this model.* Precision, parity-violating electron scattering experiments made feasible by the 12 GeV Upgrade have the sensitivity to search for deviations from the Standard Model that could signal the presence of new physics. Planned studies of the three neutral pseudoscalar mesons, the π^0, η and η', will provide fundamental information about low energy QCD, characterizing the strengths of the chiral anomalies.

This science program has expanded significantly in the two years since the project was first presented to the Nuclear Sciences Advisory Committee (NSAC) in the form of a White Paper [WP01] produced as part of the 2001-2002 NSAC Long Range Planning Process. While focusing on science, this pCDR also provides a detailed description of the required detector and accelerator upgrades so that it can serve as an overview of the entire plan for the 12 GeV project.

PREFACE

When the scientific case was made for the facility that became CEBAF, there was unanimous agreement on the importance of a continuous-beam electron accelerator but a great deal of discussion about the optimum beam energy. A subcommittee of NSAC (the Nuclear Science Advisory Committee of the U.S. Department of Energy and the National Science Foundation) chaired by Peter Barnes concluded [Ba82] that the accelerator's design energy should be 4 GeV, rather than the 2 GeV favored by some, because the higher energy would permit its experimental program "to study the largely unexplored transition between the nucleon-meson and the quark-gluon descriptions of nuclear systems". In anticipation of the future need to extend this experimental program to even higher momentum and energy transfers, the CEBAF accelerator was designed in the mid-1980s so that future extensions to energies of order 25 GeV would be straightforward.

As CEBAF's scientific program has progressed, the wisdom of these design choices has become increasingly clear. This White Paper outlines the scientific case for the upgrade of CEBAF to 12 GeV, and documents the accelerator and experimental equipment improvements necessary to carry out the scientific program. It is the result of lengthy discussions within the Jefferson Lab community that began as the 4 GeV program was just underway in the mid-1990s. In this preface we remind the reader of the main activities leading to this plan for the 12 GeV Upgrade.

As CEBAF neared completion and its experimental program was about to begin, the CEBAF User Group began an examination of the physics accessible with an upgraded CEBAF energy. This decision led to the organization of a workshop held at Jefferson Lab from 14 to 16 April 1994. It was organized into four working groups centered around four main physics topics, by an organizing committee consisting of T. Barnes, R. Ent, B. Frois, R. Holt, R. Milner, P. Mulders, J. Napolitano, M. Petratos, and P. Stoler. Each working group was represented by one or two plenary speakers who were asked to summarize the outstanding physics issues that could be addressed by an upgrade, and by many shorter parallel contributions dealing with specific issues. Members of the organizing committee then summarized their presentations and their personal views on the physics case for an upgrade of CEBAF to higher energies. The result was the "yellow book" report, *CEBAF at Higher Energies*, edited by Paul Stoler for the CEBAF User Group and Nathan Isgur for Jefferson Lab, which marked the first step toward the goal of defining the physics program that would form the basis of an upgrade of CEBAF.

The compelling science which emerged from this workshop led to a study of the upgrade options by a laboratory strategic planning group, and to two "village meetings". These studies indicated that a cost-effective upgrade of CEBAF is possible. These conclusions were presented to NSAC, which responded in the recommendations of its 1996 Long Range Plan that "the community looks forward to future increases in CEBAF's energy and to the scientific opportunities that would bring".

With this encouragement, the users held a second workshop from 15 to 18 June 1998. This

workshop, organized by Steve Dytman, Howard Fenker, and Phil Roos, was structured to review the physics motivation for the Upgrade, but to focus on the specification of the equipment and instrumentation necessary for measurements at 12 GeV. It began with plenary sessions on physics, on the issues faced by Halls A, B, and C at 12 GeV, on the preliminary designs of a new Hall D for photoproduction, and on state-of-the-art detector and polarized-source developments. Next came parallel sessions organized by physics topic on photoproduction, high-Q^2 reactions, hadrons in the nuclear medium, and inclusive and semi-inclusive reactions. These were followed by parallel sessions organized by hall. More than 180 scientists participated in the workshop; their work is recorded in *Physics and Instrumentation with 6–12 GeV Beams*, edited by the three organizers. A remarkable feature of this workshop was the quick consensus reached on the set of detectors needed to exploit the vast new physics potential of the 12 GeV Upgrade.

In anticipation of the 2001 NSAC Long Range Plan, the User Group organized a special workshop in January 2000 that was devoted to delineating the 12 GeV program for the existing experimental halls. It commissioned five follow-on working groups to develop crisp scientific cases and identify key experiments or key experimental programs in five target areas focused on these halls. Following the January workshop, at their March 2000 meeting the User Group Board of Directors appointed a White Paper Steering Committee: Lawrence Cardman, Rolf Ent, Nathan Isgur, Jean-Marc Laget, Christoph Leemann, Curtis Meyer, and Zein-Eddine Meziani.

Prior to and in parallel with this effort, the new Hall D Collaboration produced a design for a new meson photoproduction facility designed to discover and investigate the properties of gluonic excitations. Their design underwent a rigorous review in December 1999 by a distinguished external committee; the collaboration emerged from the review having received high praise for both their physics goals and their experimental design.

In 2000 the users reviewed an early draft version of this White Paper at their annual June meeting, which was once again devoted to the Upgrade. At that meeting, key experiments were selected from the many ideas that emerged from the planning for the Upgrade. These experiments were developed in greater detail, for inclusion as part of the scientific case for the Upgrade, and presented to the Jefferson Lab Program Advisory Committee at a special meeting of that committee. The PAC commented on each proposal in a manner similar to their review of research proposals for the present accelerator. In summarizing their review, the PAC noted:

> *The laboratory and the user community have developed an impressive scientific case that demands this new capability. The Jefferson Lab Program Advisory Committee was charged by the laboratory to review this science, and to review the plans for the associated experimental equipment.*
>
> *The committee concludes that an outstanding scientific case has been identified which requires the unique capabilities of the JLab 12 GeV upgrade. The results of these experiments are likely to significantly change the way we think about nuclear physics and the*

strong (nonperturbative) limit of QCD. Two major new thrusts can produce definitive results: the experimental verification of the origin of quark confinement by QCD flux tubes as predicted by lattice gauge calculations, and the determination of the quark and gluon wave functions of the nuclear building blocks. The full technical capabilities of the upgrade are required for this progress. New research domains are also opened up that show great promise in leading existing research efforts to new levels of understanding.

The proposed experimental equipment is well suited to addressing these new physics opportunities. The choices capitalize on the powerful existing equipment at the laboratory without compromising the physics goals.

The Program Advisory Committee was excited by the research potential that the 12 GeV upgrade makes possible. The scope of the upgrade is very well matched to the problems we see driving the field for the next decade. The time has come to bring these opportunities to nuclear physics.

The White Paper was improved, based on the PAC discussions, on discussion at the NSAC Long Range Plan Town Meeting held at Jefferson Lab in December 2000, and on additional community input, and a final version was published in February 2001 as a formal submission to the larger nuclear physics community as part of the Long Range Planning process.

****

White paper formed the basis of discussions of the Upgrade at the formal "resolution" meeting of the NSAC LRP held in SantaFe, NM on ***.

Comment on formal recommendations of NSAC LRP (quote).

Comment on "only one that should be done in constant effort budget"

Following the encouragement of the LRP, work began in earnest on further refining the science program and developing detailed pre-conceptual designs for the physics instrumentation.

Insert here re July 2002 Summer Workshop on the Upgrade, numberous meetings of the various hall collaboraitons, the development of four Hall-specific pCDRs (cite them all, and add as references). These documents contained extensive details on the expreimental equipment, and a presentation of the science motivating the equipment choices, incluing the developmetn of many "example" experimetns that used the equipment.

Goal of pCDR is to present the science case for the upgrade "across the halls", consolidating the physcic by topic (not surprisingly, in many of the areas of interest there are key experiments that are best done using different equipment). Also to present a condensed version of the hall equpiment to provide technical details for anyone interested in evaluating specifics.

Development (w/ UGBOD role) of the editorial board, which developed science case in a broad

variety of areas, presented it to PAC23 for review and comment, and then took responsiblity for writing.

Then presentation of updates and new science to PAC23 (1/03) for decision on the science thrusts highlighted in this pCDR. This was followed by a major writing effort by a series of subgroups:

Editorial Board was divided into groups and each group was given responsibility for text on a science or equipment topic. Specifically:

A) Gluonic Excitations and the Origin of Quark Confinement Curtis Meyer, Alex Dzierba, Ted Barnes, Carlos Salgado (and David Richards to add text re lattice)

B) Developing a Unified Description of Hadron Structure 1) Valence Quark Structure and Parton Distributions Zein-Eddine Meziani, Sebastian Kuhn, Oscar Rondon, Wally Melnitchouk

2) The Generalized Parton Distributions as Accessed via Deep(ly) Exclusive Reactions Volker Burkert, Charles Hyde-Wright, Xiangdong Ji

3) Form Factors and Polarizabilities - Constraints on the Generalized Parton Distributions Paul Stoler, Mark Jones, Bogdan Wojtsekhowski, Anatoly Radyushkin

4) Other Topics in Hadron Structure (duality, single-spin asymmetries, Q2 evolution of the GDH sum rule, etc.) Gordon Cates, Latifa Elouadrhiri, Thia Keppel, Sabine Jeschonnek

C) The Physics of Nuclei 1) Probing the Limits of the Nucleon-Based Description of Nuclei Haiyan Gao, Roy Holt, Carl Carlson Rocco Schiavilla, Larry Weinstein,and Paul Ulmer

2) The High-Density Frontier in Cold Nuclei John Arrington, Doug Higinbotham, Jean-Marc Laget, and Will Brooks

D) Symmetry Tests in Nuclear Physics 1) Standard Model Tests Paul Reimer, Mike Ramsey-Musolf, Paul Souder, and Dave Mack

2) Spontaneous Symmetry Breaking Aron Bernstein, Ashot Gasparian, Jose Goity

IV) The Experimental Equipment: A) Hall A: J.-P. Chen, Kees de Jager B) Hall B: Volker Burkert C) Hall C: Howard Fenker D) Hall D: Curtis Meyer and Alex Dzierba E) Experiment-Specific Equipment

This pCDR is based on these many workshops, their published proceedings and unpublished presentations, and on the published and unpublished work of many individuals on the physics opportunities that would open up with CEBAF at 12 GeV. A detailed draft of this document was released to the JLab User community in June 2003 to provide opportunity for community comment to be incorporated prior to the release of the final version.

The author list at the end of this document includes the names of all contributors to the effort known to us. Many of them commented extensively on the earlier drafts, resulting in a much-improved document. This White Paper would have been impossible without their intelligence, enthusiasm, time, and just plain hard work. We apologize to anyone whose contributions we have inadvertently failed to acknowledge.

The 12 GeV Upgrade pCDR Editorial Board:

John Arrington, Argonne National Lab (johna@anl.gov)
Ted Barnes, Oak Ridge National Lab (barnesfe@ornl.gov)
Aron Bernstein, Massachusetts Institute of Technology (bernstein@mitlns.mit.edu)
Will Brooks, Jefferson Lab (brooksw@jlab.org)
Volker Burkert, Jefferson Lab (burkert@jlab.org)
Lawrence Cardman, Jefferson Lab (cardman@jlab.org)
Carl Carlson, College of William & Mary (carlson@physics.wm.edu)
Gordon Cates, University of Virginia (cates@Virginia.EDU)
J.-P. Chen, Jefferson Lab (jpchen@jlab.org)
Alex Dzierba, Indiana University (dzierba@indiana.edu)
Latifa Elouadrhiri, Jefferson Lab (latifa@jlab.org)
Howard Fenker, Jefferson Lab (hcf@jlab.org)
Haiyan Gao, Duke University (gao@tunl.duke.edu)
Ashot Gasparian, North Carolina A & T/Jefferson Lab (gasparan@jlab.org)
Jose Goity, Hampton University/Jefferson Lab (goity@jlb.org)
Doug Higinbotham, Jefferson Lab (doug@jlab.org)
Roy Holt, Argonne National Lab (holt@anl.gov)
Charles Hyde-Wright, Old Dominion University (chyde@odu.edu)
Kees de Jager, Jefferson Lab (kees@jlab.org)
Sabine Jeschonnek, Ohio State University (jeschonnek.L@osu.edu)
Xiangdong Ji, University of Maryland (xji@physics.umd.edu)
Mark Jones, Jefferson Lab (jones@jlab.org)
Thia Keppel,Hampton University/Jefferson Lab (keppel@jlab.org)
Sebastian Kuhn, Old Dominion University (skuhn@odu.edu)
Jean-Marc Laget, Centre d'Etudes Nucleaire, Saclay (laget@hep.saclay.cea.fr)
Dave Mack, Jefferson Lab (mack@jlab.org)
Curtis Meyer, Carnegie Mellon University (cmeyer@ernest.phys.cmu.edu)
Wally Melnitchouk, Jefferson Lab (wmelnitc@jlab.org)
Zein-Eddine Meziani, Temple University (Meziani@vm.temple.edu)
Anatoly Radyushkin, Old Dominion University/Jefferson Lab (radyush@jlab.org)
Mike Ramsey-Musolf, California Institute of Technology (mjrm@krl.caltech.edu)
Paul Reimer, Argonne National Lab (reimer@anl.gov)
David Richards, Jefferson Lab (dgr@jlab.org)

Oscar Rondon, University of Virginia (rondon@Virginia.edu)
Carlos Salgado, Norfolk State University/Jefferson Lab (salgado@jlab.org)
Rocco Schiavilla, Old Dominion University/Jefferson Lab (schiavil@jlab.org)
Paul Souder, Syracuse University (souder@suhep.phy.syr.edu)
Paul Stoler,Rensselear Polytech Institute (stoler@rpi.edu)
Paul Ulmer, Old Dominion University (pulmer@odu.edu)
Larry Weinstein, Old Dominion University (lweinste@odu.edu)
Bogdan Wojtsekhowski, Jefferson Lab (bogdanw@jlab.org)

Contents

1 EXECUTIVE SUMMARY **1**

1.A Physics Overview 2

1.A.1 Gluonic Excitations and the Origin of Quark Confinement 3

1.A.2 The Fundamental Structure of the Nuclear Building Blocks 8

Form Factors - Constraints on the Generalized Parton Distributions 11

Valence Quark Structure and Parton Distributions 13

The Generalized Parton Distributions as Accessed via Deeply Exclusive Reactions 15

Other Topics in Hadron Structure 17

Transverse parton distributions 19

The extended GDH integral and sum rule 19

Duality: the transition from a hadronic to a quark-gluon description of Deep Inelastic Scattering 19

1.A.3 The Physics of Nuclei 20

The Short-Range Behavior of the $N-N$ Interaction and Its QCD Basis . . . 21

Color transparency. 22

Learning about the NN force by the measurement of the threshold ψN cross section and by searching for ψ-nucleus bound states. 22

Quark propagation through cold QCD matter: nuclear hadronization and transverse momentum broadening. 23

Short-range correlations in nuclei: the nature of QCD at high density and the structure of cold, dense nuclear matter. 23

Identifying and Exploring the Transition from the Meson/Nucleon Description of Nuclei to the Underlying Quark and Gluon Description. . . . 25

The onset of scaling behavior in nuclear cross sections 25

Helicity conservation in nuclear reactions . . . 27
The charged pion form factor . . . 27
Pion photoproduction off the nucleon and in the nuclear medium . . . 27
1.A.4 Symmetry Tests in Nuclear Physics . . . 28
Standard Model Tests . . . 28
Properties of Light Pseudoscalar Mesons via the Primakoff Effect . . . 30
1.B Upgrade Project Summary . . . 32
1.B.1 The Accelerator . . . 33
1.B.2 The Experimental Equipment . . . 35
Hall A and the Medium Acceptance Device (MAD) . . . 35
Hall B Upgrade and CLAS^{++}. . . . 37
Hall C and the Super High Momentum Spectrometer (SHMS) . . . 40
Hall D and the GlueX Experiment . . . 44

2 THE SCIENCE DRIVING THE 12 GeV UPGRADE OF CEBAF 47

2.A Gluonic Excitations and the Origin of Quark Confinement . . . 47
2.A.1 Introduction . . . 47
2.A.2 Conventional light mesons . . . 50
2.A.3 Gluonic excitations and confinement . . . 53
2.A.4 Observation of gluonic excitations . . . 55
Glueballs . . . 55
Exotic hybrid mesons . . . 56
2.A.5 Photoproduction of exotic hybrids . . . 59
Why photoproduction? . . . 59
Current photoproduction data . . . 60

2.A.6 Complementarity with other searches 62
2.A.7 Production and analysis of hybrid mesons 63
Kinematics 63
PWA requirements 64
Linear polarization of the beam 65
Linear and circular polarization 65
Linear polarization and statistics 65
Linear polarization and production mechanism 66
Linear polarization as an exotics filter 66
2.B The Fundamental Structure of the Nuclear Building Blocks 67
2.B.1 Form Factors – Constraints on the Generalized Parton Distributions 67
Introduction 67
Form Factors at Large Momentum Transfer 70
Form Factors and Generalized Parton Distributions 71
Baryon Form Factors and GPDs 74
pQCD - Constituent Scaling, Helicity Conservation 83
Summary 85
2.B.2 Valence Quark Structure and Parton Distributions 86
Theoretical predictions for large-x distributions 89
The structure of the free neutron 91
"Tagged" neutron structure function 91
Deep inelastic scattering from $A = 3$ nuclei 91
Longitudinal–transverse separation 93
Moments of structure functions 94

The spin structure of the nucleon . . . 96
Neutron spin structure functions . . . 96
Higher-twist effects . . . 99
Semi-inclusive scattering . . . 102
2.B.3 The Generalized Parton Distributions as Accessed via Deeply Exclusive Scattering . . . 106
The Physics of the Generalized Parton Distributions . . . 106
Spin Structure of the Nucleon . . . 109
Gravitational Form Factors . . . 109
"Tomographic" Images of the Nucleon . . . 110
Modeling GPDs . . . 111
Probing GPDs Through 12 GeV Upgrade . . . 111
DVCS at JLab with 12 GeV Electrons . . . 115
Deeply Virtual Meson Production at JLab with 12 GeV Electrons . . . 123
From Observables to GPDs . . . 131
2.B.4 Other Topics in Hadron Structure . . . 132
Transverse parton distributions . . . 132
The extended GDH integral and sum rule . . . 137
Quark-Hadron Duality . . . 139
2.C The Physics of Nuclei . . . 144
2.C.1 Hadron Structure in the Nuclear Medium . . . 146
Nuclear Matter at High Densities . . . 148
Modification to Hadron Structure in Nuclei . . . 149
High-Density Configurations in Nuclei . . . 150
Color Transparency . . . 153

Color Transparency in A(e,e'p) . . . 153
Color Transparency in Few-Body Systems . . . 154
Color Transparency in Meson Production . . . 156
J/ψ Photoproduction Near Threshold . . . 157
Space-Time Characteristics of Hadronization . . . 161
Transverse Momentum Broadening . . . 165
2.C.2 Short-Range Correlations in Nuclei . . . 166
Electrodisintegration of the Deuteron . . . 167
$A(e, e'pN)$ Processes . . . 169
Inclusive $A(e, e')X$ Processes . . . 170
2.C.3 The Parton-Hadron Transition in Nuclei . . . 173
Elastic Form Factor of Charged Pion . . . 174
Few-Body Form Factors . . . 175
Deuteron Photodisintegration . . . 177
Nucleon Photopion Production . . . 178
Pion Photoproduction in the Nuclear Medium . . . 182
2.D Symmetry Tests in Nuclear Physics . . . 184
2.D.1 Standard Model Tests . . . 184
2.D.2 Properties of Light Pseudoscalar Mesons via the Primakoff Effect . . . 195

3 EXPERIMENTAL EQUIPMENT FOR THE 12 GeV UPGRADE 208

3.A Hall A and the Medium Acceptance Device (MAD) . . . 208
3.A.1 Design Characteristics of the MAD Spectrometer . . . 210
3.A.2 Optical Characteristics of the MAD Spectrometer . . . 220
3.A.3 Simulations of the MAD Spectrometer . . . 222

3.A.4 MAD Spectrometer Detector Systems . . . 226
Scintillators . . . 227
Drift Chambers . . . 229
Gas Čerenkov Counter . . . 230
Aerogel Čerenkov Counters . . . 232
Electromagnetic Calorimeter . . . 232
Focal Plane Proton Polarimeter . . . 234
Trigger Electronics . . . 235
Data Acquisition . . . 236
3.A.5 High Performance Calorimeter . . . 237
3.A.6 The Hall A Beam Line . . . 239
3.B Hall B Upgrade and the CLAS^{++} Detector . . . 241
3.B.1 Overview . . . 241
3.B.2 CLAS Torus Magnet . . . 243
3.B.3 Central Detector . . . 244
Superconducting Solenoid Magnet . . . 245
Magnet Design . . . 245
Central Electromagnetic Calorimeter . . . 246
Overview . . . 246
Requirements . . . 247
Scintillating Fiber/Tungsten Powder Calorimeter Design . . . 247
Expected Performance . . . 248
Prototyping and Simulations . . . 250
Central Time-of-Flight System . . . 251

Expected Rates . . . 251
Options . . . 253
Central Tracker . . . 253
Silicon Strip Detector . . . 255
Instrumentation . . . 256
Prototyping . . . 257
Forward Detector . . . 257
Overview . . . 257
High Threshold Čerenkov Counter (HTCC) . . . 259
Forward Tracking Chambers . . . 260
Low Threshold Čerenkov Counter . . . 262
Outer TOF System . . . 262
Inner Calorimeter . . . 265
Forward Angle Calorimeter . . . 266
Pre-shower calorimeter . . . 267
3.B.4 Polarized Target Operation in CLAS^{++} . . . 268
Longitudinally polarized Target in Solenoid Magnet . . . 268
Transversely Polarized Target. . . . 270
3.B.5 Beam Line . . . 270
Faraday Cup . . . 270
Møller Polarimeter . . . 271
Magnetic Chicane . . . 271
Beam raster magnets . . . 271
3.B.6 Data Acquisition System and Trigger . . . 271

Design criteria for the system . . . 271
System upgrade . . . 272
3.B.7 Event Reconstruction and Offline Computing . . . 272
Data Reduction and Online Event Reconstruction . . . 273
3.C Hall C and the Super High Momentum Spectrometer (SHMS) . . . 274
3.C.1 Overview . . . 274
3.C.2 The High-Momentum Spectrometer . . . 274
3.C.3 The Super-High-Momentum Spectrometer . . . 277
Overview . . . 277
The SHMS Magnets and Structural Design . . . 278
General . . . 278
Q1 at 8.6 T/m . . . 279
QD30 Superconducting Magnet for the SHMS . . . 280
Magnet DC Power and Energy Dump System . . . 282
Magnet Control System . . . 285
Support Structure . . . 286
Spectrometer Motion System . . . 286
Shield House . . . 288
SHMS Cryogenic System . . . 288
SHMS Vacuum Systems . . . 289
SHMS Optics and Monte Carlo . . . 290
SHMS Optics Design . . . 290
COSY magnet model . . . 292
LSA tune . . . 294

SHMS model in the 'physics' Monte Carlo 295
SHMS Performance (Resolution/Acceptance) 297
SHMS Detector Systems 298
Wire Chambers 303
Quartz Čerenkov Hodoscope 305
Particle Identification 309
Focal Plane Polarimeter 320
Trigger, Data Acquisition, and On-line Computing 320
Stand-Alone (Third-Arm) Calorimeter 322
3.D Hall D and the GlueX Experiment 323
3.D.1 Introduction 323
3.D.2 The Photon Beam and Polarization 323
The Photon Tagger and Beam Collimation 324
Polarization via Coherent Bremsstrahlung 325
3.D.3 The GlueX Detector 327
The Super-conducting Solenoid 327
Particle Tracking and Particle Identification 328
The Vertex Detector 328
The Cylindrical Drift Chamber 329
The Forward Drift Chambers 330
Electromagnetic Calorimetry 331
The Forward Calorimeter 331
The Barrel Calorimeter 332
The Upstream Photon Veto 334

Charged Particle Identification 335
The Time-of-Flight System 335
The Čerenkov Detector 337
Sub-system Installation and Integration 338
3.D.4 Rates, Electronics, Trigger and Data Acquisition 338
3.D.5 Computing and Partial Wave Analysis 342
3.D.6 Summary 347
3.E Experiment-Specific Equipment 347
3.E.1 Properties of Light Pseudoscalar Mesons via the Primakoff Effect 347

REFERENCES **357**

FIGURES **386**

TABLES **398**

CONTRIBUTORS TO THE pCDR **400**

1 EXECUTIVE SUMMARY

There has been a remarkably fruitful evolution of our picture of the behavior of strongly interacting matter during the almost two decades that have passed since the parameters of the Continuous Electron Beam Accelerator Facility (CEBAF) at Jefferson Lab were defined. These advances have revealed important experimental questions best addressed by a CEBAF-class machine at higher energy. Fortunately, favorable technical developments coupled with foresight in the design of the facility make it feasible to triple CEBAF's beam energy from the original design value of 4 GeV to 12 GeV (corresponding to doubling the achieved energy of 6 GeV to 12 GeV) in a cost-effective manner: the Upgrade can be realized for a modest fraction of the cost of the initial facility. This Upgrade would provide the worldwide community using CEBAF with greatly expanded physics horizons.

Raising the energy of the accelerator to 12 GeV provides three general advantages:

1. It allows crossing the threshold above which the origins of quark confinement can be investigated. Specifically, 12 GeV will enable the production of certain "exotic" mesons, whose discovery and spectrum will establish the origin of quark confinement as due to the formation of QCD flux tubes and whose spectrum encodes information on the mechanism within QCD responsible for their formation. If these exotic mesons are not found their absence will present a serious challenge to our present understanding of "strong" QCD, and the meson spectra that will be accumulated with unprecedented statistics (including spectra of mesons containing strange quarks and antiquarks) will provide essential information for revising that theory. With 12 GeV one also crosses the threshold for charmed meson production.

2. It allows direct exploration of the quark-gluon structure of hadrons and nuclei. It is known that inclusive electron scattering at the high momentum and energy transfers available at 12 GeV is governed by elementary interactions with quarks and gluons. The design energy of the original CEBAF accelerator has proven to be not fully adequate for study of this critical regime. This is not unexpected; at the time the energy was chosen, among other things, to "just" get into the deep inelastic scattering regime. With continuous 12 GeV beams one can cleanly access hadron structure throughout the entire "valence quark region" and exploit the newly discovered Generalized Parton Distributions to access experimentally both the correlations in the quark wavefunctions of the hadrons and their transverse momentum distributions. 12 GeV beams will allow us to identify precisely the limits of the long-standing nucleon and meson based description of nuclei, and to fully access and characterize the transition from this description to the underlying quark-gluon description

3. In addition to these qualitative changes in the physics reach of CEBAF, the 12 GeV Upgrade also allows important new thrusts in CEBAF's present research program, generally involving the extension of measurements to substantially higher momentum transfers (probing corre-

spondingly smaller distance scales). We also note that most experiments that want to run at a presently accessible momentum transfer can do so more efficiently (*e.g.*, consuming less total beam time) at higher electron beam energy.

In the examples highlighted in this executive summary and in the more complete discussions of Chapter 2, these benefits of the energy upgrade will always be significant.

1.A Physics Overview

Chapter 2 provides a detailed discussion of the science motivation driving the 12 GeV Upgrade; it is summarized here. The research program of the new facility is focused on four major research themes that coincide with broad directions of the field of nuclear physics as identified in two key documents: the 2002 Long Range Plan [NS02] of the Nuclear Science Advisory Committee of the U.S. Department of Energy and the National Science Foundation and the recent decadal survey [NA99] of the field by the National Research Council of the National Academy of Sciences. We identify these themes here to place our research program in this broader context. Each addresses outstanding questions in nuclear physics that the laboratory's users address with a concerted program of experimental and theoretical work.

Gluonic Excitations and the Origin of Quark Confinement
Experiments and theory aimed at examining the fundamentally new dynamics that underpins all of nuclear physics: the confinement of quarks.

How are the Nuclear Building Blocks Made from Quarks and Gluons?
A program of measurements addressing the first question that must be answered in the quest to understand nuclear physics in terms of the fundamental theory of strongly interacting matter: quantum chromodynamics (QCD).

On the Structure of Nuclei
Three broad programs that take advantage of the precision, spatial resolution, and interpretability of electromagnetic interactions to address long-standing issues in nuclear physics. They aim to understand the QCD basis of nuclear physics through investigations of the origins of the Nucleon–Nucleon ($N-N$) force and its short range behavior, and by identifying and exploring the transition from the meson/nucleon description of nuclei to the underlying quark and gluon description.

In Search of the New Standard Model
Experiments aimed at identifying physics beyond the Standard Model of electro-weak interactions through precision tests of its predictions, and by measuring low energy parameters of the theory to deepen our understanding of chiral symmetry breaking.

Each of these programs is a major motivation for the energy upgrade. The first, a program of *gluonic spectroscopy*, will provide data needed: i) to test experimentally our current understanding that quark confinement arises from the formation of QCD flux tubes; and ii) to explore the mechanism

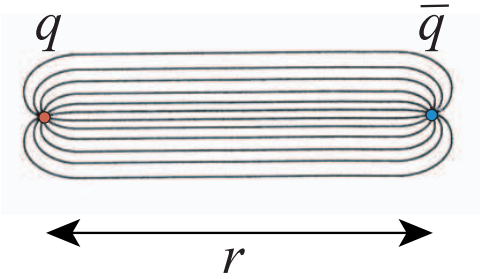

Figure 1: In QCD a confining flux tube forms between distant static charges. The Hall D program is designed to verify this fundamental new feature of chromodynamics.

behind the formation of these flux tubes. If our present understanding is incorrect, the experiment has the sensitivity necessary to decisively test first-principles lattice QCD calculations of the mesons – the simplest of the strongly-interacting systems. The second program will explore the *complete quark and gluon wavefunctions* of the nucleons through measurements: i) of quark momentum distributions in the critical, but previously unreachable, valence quark region; and ii) of exclusive reactions that build on the framework of the newly discovered Generalized Parton Distributions. The third will address outstanding issues in nuclear physics, completing a very fruitful area presently under investigation with CEBAF at 6 GeV and extending this program in important new directions. Finally, the last program will use precision measurements at modest energies to explore the validity of the Standard Model of electro-weak interactions and measure key parameters of that theory. In Sections 1.A.1 through 1.A.4 we summarize these four key science drivers of the 12 GeV Upgrade. Section 1.B then completes the picture by summarizing the accelerator and experimental equipment upgrades required to accomplish these physics goals.

1.A.1 Gluonic Excitations and the Origin of Quark Confinement

In the early 1970s, evidence that the masses of strongly interacting particles increased without limit as their internal angular momentum increased led the theorist Yoichiro Nambu [Na70] to propose that the quarks inside these particles are "tied together" by strings. Numerical simulations of QCD ("lattice QCD") have demonstrated [Ba00] that Nambu's conjecture was essentially correct: in chromodynamics, a stringlike chromoelectric flux tube forms between distant static quarks, leading to their confinement with an energy proportional to the distance between them (see Figs. 1 and 2). The phenomenon of confinement is the most novel and spectacular prediction of QCD – unlike anything seen before. It is also the basic feature of QCD that underpins nuclear physics, from the mass of the proton and other nuclear building blocks to the NN interaction.

The ideal experimental test of this new feature of QCD would be to study the flux tube directly by anchoring a quark and antiquark several fermis apart and examining the flux tube that forms between them. In such ideal circumstances one of the fingerprints of the gluonic flux tube would be

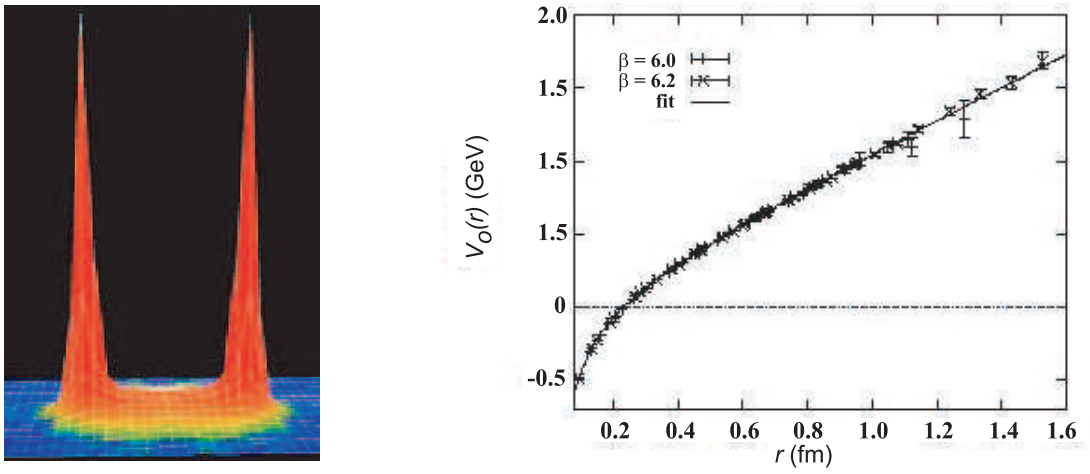

Figure 2: Lattice QCD has confirmed the existence of flux tubes between distant static charges for heavy quarks. In addition to the intense color fields in the immediate vicinity of each quark, one can see the formation [Ba00] along the line connecting the two quarks of a flux tube of constant thickness, leading to the linearly rising potential seen on the right [Ba97].

its model-independent spectrum [Lu81] (see Fig. 3): its required two degenerate first excited states are the two longest-wavelength vibrational modes of this system, while their excitation energy is required to be π/r since both the mass and the tension of this "relativistic string" arise from the energy stored in its color force fields. Such a direct examination of the flux tube is of course not possible experimentally, but such a picture is indicated by lattice calculations, at least at large separations [Ju02]. In real life we have to be content with systems in which the quarks move. Fortunately, we know both from general principles [Is85] and from lattice QCD calculations [Ju99] that an approximation to the dynamics of the full system that ignores the impact of these two forms of motion on each other works quite well – at least down to quark masses of the order of 1 GeV.

To extend this firm understanding to yet lighter quarks, models are required [Is85], but the most important properties of this system are determined by the model-independent features described above. In particular, in a region around 2 GeV, a new form of hadronic matter must exist in which the gluonic degree-of-freedom of a quark-antiquark system is excited. The smoking gun characteristic of these new states is that the vibrational quantum numbers of the gluonic "string", when added to those of the quarks, can under certain circumstances produce a total angular momentum J, a total parity P, and a total charge conjugation symmetry C not allowed for ordinary $q\bar{q}$ states. These unusual J^{PC} combinations (such as 0^{+-}, 1^{-+}, and 2^{+-}) are called exotic, and the states are referred to as exotic hybrid mesons [Ba77]. Not only general considerations and flux tube models, but also first-principles lattice QCD calculations, require that these states have masses around 2 GeV; furthermore, they demonstrate that the levels and their orderings will provide experimental information on the mechanism that produces the flux tube.

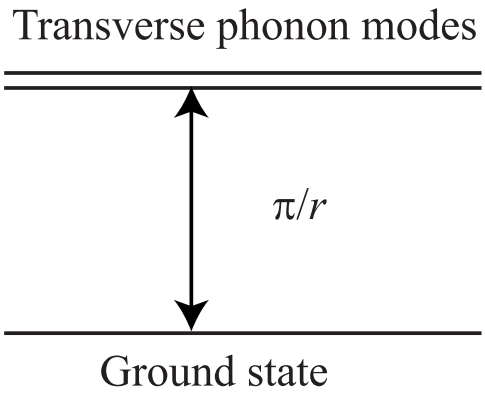

Figure 3: Model-independent spectrum of the glue (flux tube) of Fig. 1.

On the experimental front, tantalizing evidence has appeared in recent years both for exotic hybrids and for glueballs (gluonic excitations with no quarks). For the last two years a group of 90 physicists from 26 institutions in seven countries has been working on the design of the definitive experiment to map out the spectrum of these new states required by the confinement mechanism of QCD. Photon beams are expected to be particularly favorable for the production of the exotic hybrids [Is85]. The reason is that the photon can easily fluctuate into a "virtual vector meson" with total quark spin $S = 1$.

When the flux tube in this $S = 1$ system is excited, both ordinary and exotic J^{PC} are possible. In contrast, when the spins are antiparallel ($S = 0$), as in pion or kaon probes, the exotic combinations are not generated. (In the approximation that flux tube and quark dynamics separate, hybrid production would occur by pure flux tube excitation, and these selection rules would be strictly true. In practice, these two degrees-of-freedom interact with one another to produce corrections to the rules.) To date, most meson spectroscopy has been done with incident pion, kaon, or proton probes, so it may not be surprising that the experimental evidence to date for flux tube excitation is tentative.

In contrast to hadron beams, high-flux photon beams of sufficient quality and energy to perform meson spectroscopy studies have not been available, so there are virtually no data on the photoproduction of mesons with masses in the 1.5 to 3 GeV region. Thus, experimenters have not been able to search for exotic hybrids precisely where they are expected to be found. The planned experiment will have a dramatic impact on this situation. Even if initial running is at only 10% of the planned photon fluxes of 10^8/s, the experiment will accumulate statistics during the first year of operation that will exceed the world's supply of published meson data obtained by pion production by at least a factor of 10, and the existing photon production data set by at least a factor of 1000. With the planned detector (described below), high statistics, and linearly polarized photons, it will be possible to map out the full spectrum of the decay modes of these gluonic excitations.

The GlueX experiment is complementary to the recently approved CLEO-c program at Cornell, which will include the collection of nearly one billion J/ψ decays. The radiative J/ψ decays are expected to be glue-rich, the system recoiling against the radiated photon having the quantum numbers of a two-gluon system. Thus the glueball search of CLEO-c is complementary to the hybrid search of GlueX and while GlueX is not ideal for glueball searches, CLEO-c is not ideal for exotic hybrid searches. In addition, GlueX and CLEO-c physicists are working together to develop the software and analysis tools needed to perform the spin analysis of the large datasets expected in both experiments. The complete mapping of the spectrum of gluonic excitation in these programs will the definitive data needed to understand confinement.

The performance of the GlueX detector and the flux and linear polarization of the photon beam determine the level of sensitivity for mapping the hybrid spectrum. A double-blind exercise was carried out in which an exotic signal, a $J^{PC} = 1^{-+}$ state with a mass of 1.6 GeV/c^2 decaying into $\rho\pi$, was generated along with a mix of three well-established non-exotic states with masses of 1.2, 1.3 and 1.7 GeV/c^2. In this exercise the exotic signal was generated at the level of 2.5% of the total sample. The momenta of the decay products of these particles were smeared according to the expected resolution of the detector. The acceptance of the detector was also applied. The resulting data set was passed through a partial wave analysis (PWA) fitting procedure to determine the relative contributions of each wave. The plot in Fig. 4 shows the input exotic wave as a solid curve and the result of the PWA fit as points with error bars. The input wave is reproduced extremely well, and this demonstrates the capabilities of the detector and sensitivity of the experiment. The experiment is described in Section refsubsec:halld; a much more complete discussion of the physics driving the experiment is given in Section 2.A.

When the spectrum and decay modes of these gluonic excitations have been mapped out experimentally, we will have made a giant step forward in understanding one of the most important phenomena discovered in the twentieth century: quark confinement.

The data that will be accumulated as part of the search for gluonic excitation will also provide new information on the spectroscopy of $s\bar{s}$ mesons that is essential for completing our understanding of QCD. The left half of Fig. 5 shows some of what we know about the spectra of $Q\bar{q}$ mesons for $\bar{q}$ a light ($\bar{d}$) quark and $Q = b, c, s$, and u. The rigorous results of Heavy Quark Effective Theory (HQET) should only be applicable for $Q = b, c$, but these data suggest that there is a remarkable similarity between the dynamics of "true" heavy-light systems and those where $Q = s$ or even $Q = u$ or d. It appears that the creation of the constituent quark mass through spontaneous chiral symmetry breaking is enough to boost any quark into the heavy-quark world, at least qualitatively. The right half of Fig. 5 shows heavy quarkonia ($Q\bar{Q}$ systems) starting from the heaviest $b\bar{b}$ system to the lightest. Once again, even though there is no known rigorous explanation, there seems to be a great similarity between the spectra of the heavy quarkonia (which have a well-understood quark-model-like connection to QCD) and light-quark systems.

These interesting data showing possible relationships between heavy- and light-quark systems

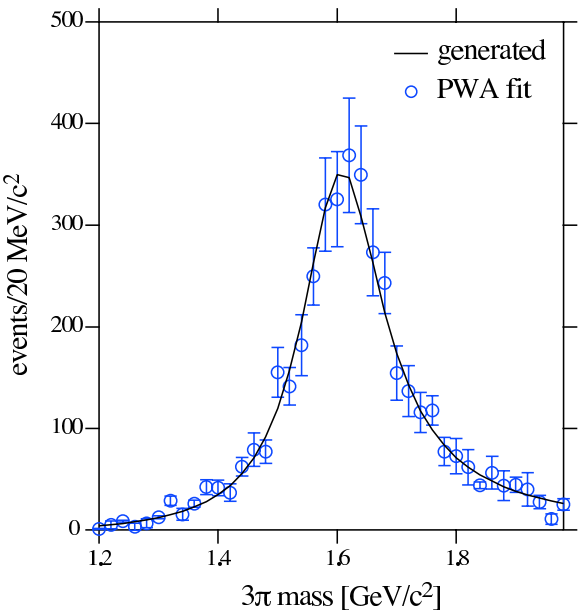

Figure 4: The results of a double-blind Monte Carlo exercise showing the $J^{PC} = 1^{-+}$ exotic wave after fitting (open circles) and the exotic wave input (curve) into the mix of $\gamma p \to \pi^+\pi^+\pi^- n$ events that were generated in this study.

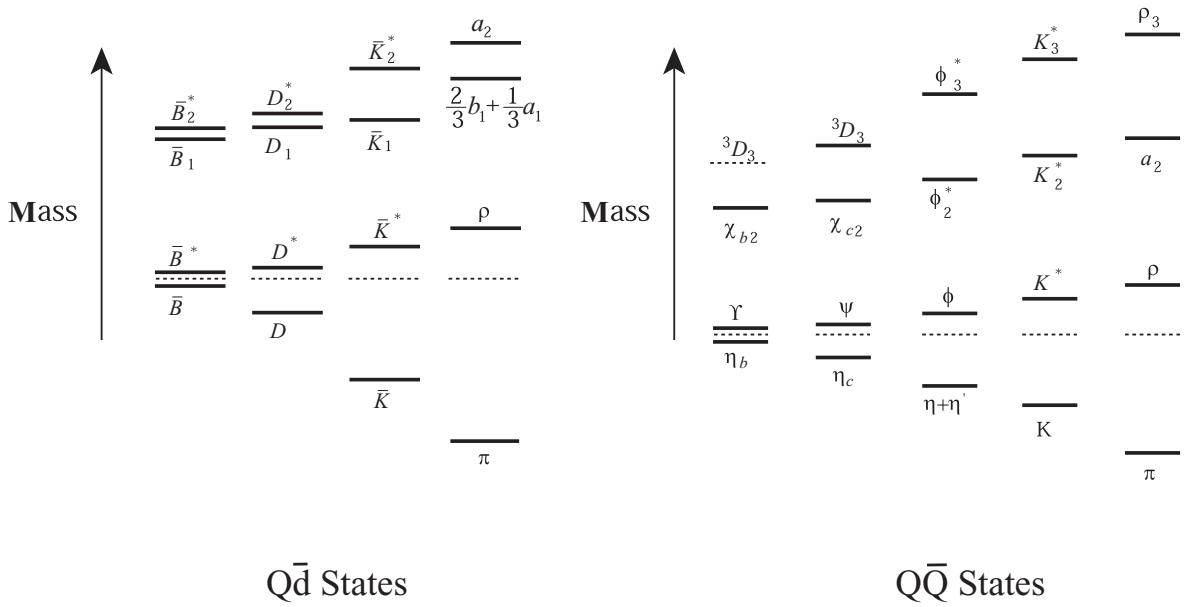

Figure 5: (Left) The relative splittings of the $Q\bar{d}$ states are shown to scale from the heaviest to the lightest with the center-of-gravity of the ground state multiplets aligned: $b\bar{d}$, $c\bar{d}$, $s\bar{d}$, and $u\bar{d}$. $\bar{B}^*$ and $\bar{B}$ are the $J^P = 1^-$ and 0^- "ground state" multiplet with light-degrees-of-freedom spin-parity $s_\ell^{\pi_\ell} = \frac{1}{2}^+$, while $\bar{B}_2^*$ and $\bar{B}_1$ with $J^P = 2^+$ and 1^+ are an excited heavy-quark spin multiplet with $s_\ell^{\pi_\ell} = \frac{3}{2}^+$ [Is91]. (Right) The $Q\bar{Q}$ states are shown from the heaviest to the lightest: $b\bar{b}$, $c\bar{c}$, $s\bar{s}$, $s\bar{d}$, and $u\bar{d}$. Shown are the states in each sector with $J^{PC} = 0^-, 1^-, 2^+$, and 3^-; relative splittings are shown to scale with the center-of-gravity of the "ground states" 0^- and 1^- aligned.

exist because nature has presented us with an interesting selection of quark masses. Historically the quarks have been divided into two groups based on their masses: the light-quark (u, d) world (or, by extension, the u, d, s world of SU(3)) and the heavy-quark world. It is ironic that in many critical areas we know much more (both experimentally and theoretically) about the heavy-quark world than we know about our own world. In this respect, these figures strongly suggest that it would be desirable to know much more about $s\bar{s}$ spectroscopy. Given that the photon often fluctuates into an $s\bar{s}$ pair, a great deal of data will automatically be available from this sector as part of the planned exotic meson program, creating the opportunity to correct this situation. Mapping out the $s\bar{s}$ spectrum presents some challenges. Given that the intrinsic $s\bar{s}$ content of the proton is expected to be small, photon-initiated $s\bar{s}$ spectroscopy will strongly favor the production of diffractive-type $C = -1$ states. The exception will be channels where OZI-violating t-channel exchanges (like those of the $\eta - \eta'$ system) can occur. These effects will result in an uneven population of the spectrum. The very high data rates anticipated should nevertheless lead to a data set of sufficient quality that the weakly excited states will still be identifiable.

1.A.2 The Fundamental Structure of the Nuclear Building Blocks

The nucleons are the basic building blocks of atomic nuclei. Their internal structure, which arises from their quark and gluon constituents, determines their mass, spin, and interactions. These, in turn, determine the fundamental properties of the nuclei. To make further progress in our understanding of nuclei, it is crucial that we understand in detail how the nucleon's basic properties are derived from the theory of strong interactions: quantum chromodynamics (QCD).

Over the past half century much progress has been made toward unraveling the structure of the nucleon. However, our understanding is fragmented and incomplete, and many puzzles remain. For example, we only partially understand how the nucleon's spin is "assembled" from the quark spins and the quark and gluon angular momenta, and we don't know the details of the spatial and momentum distributions of the quarks and gluons within the nucleon. Our understanding of nucleon structure is, quite simply, very far from the level of our understanding of atomic structure.

The JLab 12 GeV Upgrade will support a great leap forward in our knowledge of hadron structure through major programs in three areas: nucleon form factors at large Q^2, valence quark structure, and deep exclusive scattering. It will also support important initiatives in a number of other areas of hadron structure. These data can be understood and interpreted coherently, using the theoretical framework of the recently-discovered Generalized Parton Distributions (GPDs), to provide truly remarkable and revealing images of the proton's structure that will enable us to understand these fundamental "building blocks" of nuclear physics.

Nucleon Form Factors at Large Q^2. Historically, the internal structure of the nucleons was first studied by using elastic electron-proton scattering in which a proton at rest is struck by

a virtual photon of mass^2 Q^2, and the probability that the proton remains intact is measured. This elastic form factor can be directly related to the nucleon's spatial electric charge and current distributions. The first measurements of the proton's electric form factor taught us that the nucleon has a finite size of about one femptometer (10^{-15}m); Robert Hofstadter was awarded the Nobel prize for this discovery. Form factors at large Q^2 are difficult to measure because they require a dedicated accelerator with high luminosity. For many years after Hofstadter's initial measurements there were no further fundamental breakthroughs in our understanding of the nucleon because no appropriate facility was available.

The theoretical understanding of the form factors has expanded significantly. It was realized that they can be interpreted as the Fourier transformations of charge and current (or quark) density distributions in the transverse plane. This is similar to the Feynman parton distribution, which can be interpreted in a frame of reference in which the nucleon travels with the speed of light.

Parton Distributions at Large x. A second window on nucleon structure came with the development of deep inelastic lepton-nucleon scattering (DIS) in the 1970s at SLAC. In these experiments the hadronic reaction products are not detected. DIS data led to the experimental confirmation of the existence of quarks and helped to establish QCD as the fundamental theory governing all strongly interacting (*i.e.*, nuclear) matter. Friedman, Kendall, and Taylor won the Nobel prize for pioneering this research.

What one infers from DIS data are the quark distributions in momentum space. In frames of reference in which the nucleon travels with speed approaching the velocity of light, the DIS cross sections determine the probability of the struck quark having a fraction, x, of the nucleon's longitudinal momentum. In such situations the elastic form factors and the deep-inelastic structure functions provide complementary information. The former gives the coordinate space distribution in the transverse direction, and the latter yields the momentum space distribution in the longitudinal direction. Together, they provide parts of a 3-dimensional picture of nucleon structure.

Even though DIS experiments have been pursued vigorously for nearly 30 years, it is remarkable that there has never been an experimental facility that could measure the DIS cross sections throughout the kinematic regime where the three basic ("valence") quarks of the proton and neutron dominate the wavefunction. The contribution of the valence quarks peaks at $x \simeq 0.2$. However, if one is in the conventionally defined deep inelastic regime, the probability of finding a quark in the high-x "valence quark region" is small, and becomes smaller and smaller as $x \to 1$. Moreover, with "pollution" from gluons and quark-antiquark pairs, it is only for $x > 0.5$ that the valence quarks dominate the wavefunction. The 12 GeV Upgrade will allow us to map out the quark distribution functions in this "clean" valence quark region with high precision. Such measurements will have a profound impact on our understanding of the structure of the proton and neutron.

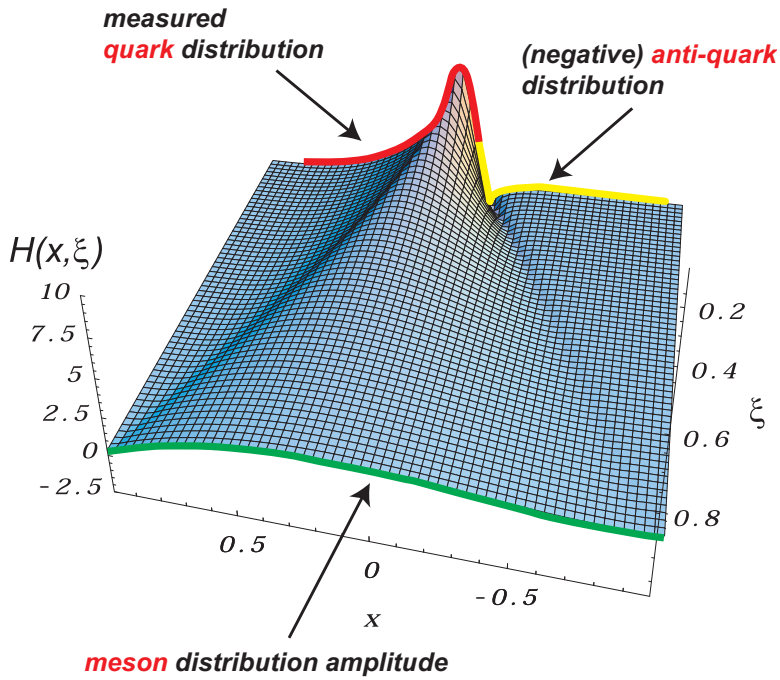

Figure 6: Model representation of the Generalized Parton Distribution (GPD) $H(x, \xi, t = 0)$ in two dimensions. The known parton momentum densities constrain the distribution at $\xi = 0$. The new physics is contained in the ξ- and t-dependence of this surface, which can currently only be modeled. The dramatic change in the shape of the surface reflects changes in the underlying physics. As ξ increases, the correlations between the quarks and anti-quarks increase leading to meson-like distributions at large ξ.

Deep Exclusive Scattering and the Generalized Parton Distributions While the elastic form factors and parton distributions provide the distributions of quarks in the transverse coordinate and longitudinal momentum spaces, respectively, they do not yield a complete picture. To have this, one would need a joint distribution representing the density of quarks having a fixed longitudinal momentum and *simultaneously* a fixed transverse position. Such a distribution has been discovered recently: the Generalized Parton Distribution (GPD) [Mu94, Ji97, Ra96].

A GPD depends on three kinematic variables: x, which specifies the fraction of the nucleon momentum carried by partons (as in the Feynman distribution); t, which characterizes the momentum transfer to the nucleon (as in the elastic form factors); and ξ, which measures the difference in momentum fraction between the initial and final parton. When $t = \xi = 0$, a GPD reduces to a regular Feynman parton distribution; when integrated over x the GPD gives an ordinary electromagnetic form factor. There are eight GPDs for each quark flavor. For example, $H(x, \xi, t)$ and $E(x, \xi, t)$ are quark helicity-independent distributions, and $\tilde{H}(x, \xi, t)$ and $\tilde{E}(x, \xi, t)$ are helicity-dependent distributions. A model of the H distribution with factorized t-dependence is shown in Fig. 6. At $\xi = 0$, the physical interpretation of $H(x, 0, t)$ is very simple [Be02], as illustrated in Fig. 7. Its Fourier transformation in t gives the joint probability distribution for a quark with longitudinal momentum x and transverse position $b_\perp$.

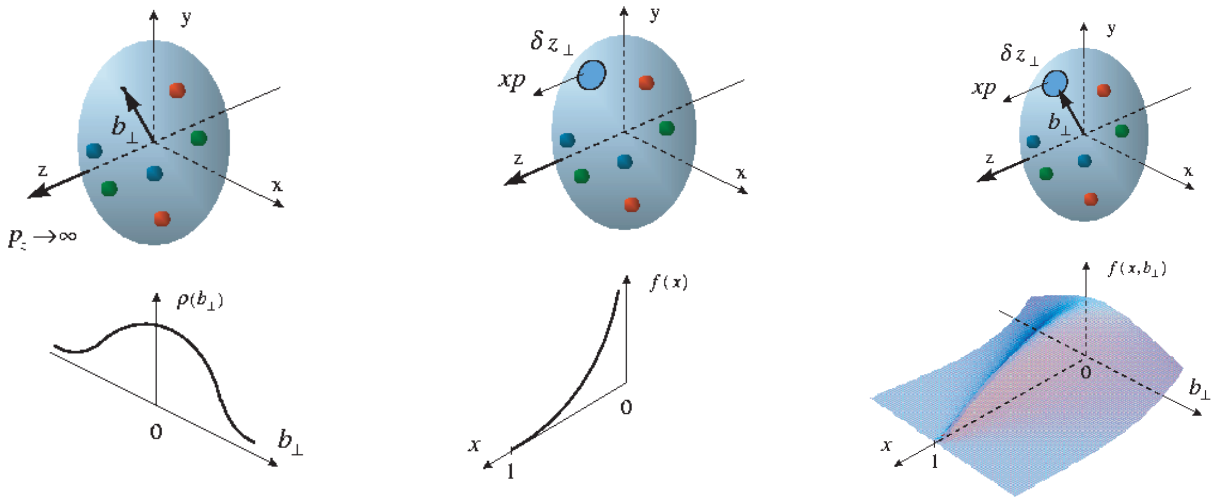

Figure 7: Representations of the proton properties probed in elastic scattering (left), deeply inelastic scattering (center), and deeply exclusive scattering (right). Elastic scattering measures the charge density $\rho(b_\perp)$ as a function of the transverse coordinate $b_\perp$. DIS measures the longitudinal parton momentum fraction density $f(x)$. GPDs measure the full correlation function $H(x, b_\perp)$.

These remarkable functions capture the full richness of the nucleon's structure. In addition to providing a consistent theoretical framework for interpreting a broad variety of available data probing nucleon structure, they provide critically needed access to essential, but almost unknown aspects of nucleon structure such as the correlations among the quarks and the quarks' contribution to the nucleon's spin. In the remainder of this section we discuss the advances anticipated in each of the important areas of nucleon structure studies that will be supported by the 12 GeV Upgrade.

Form Factors - Constraints on the Generalized Parton Distributions The hadronic form factors are moments of the GPDs; they provide precise information on the distribution of charge and magnetization in protons, neutrons and nuclei, and are essential tests of our understanding of nucleon structure. Using the formalism of the GPDs outlined above (and discussed below), elastic and transition form factors can be connected directly to the parton structure of the hadrons. They are complementary to deeply virtual exclusive (DVE) reactions (discussed below), which probe the GPDs more directly; the form factors uniquely access the GPD moments independent of skewedness. Another important consideration is that while DVE reactions access GPDs only at relatively low $|t|$, the form factors connect at high $|t|$ ($=Q^2$ for elastic scattering). High-Q^2 data are required to obtain the small $b_\perp$ structure of the hadron.

For nucleon elastic scattering there are four form factors – two for the proton (G_E^p and G_M^p), and two for the neutron (G_E^n and G_M^n); taken together they determine the charge and current distributions of the nucleon. They are the first moments of the GPDs. It is important to extend

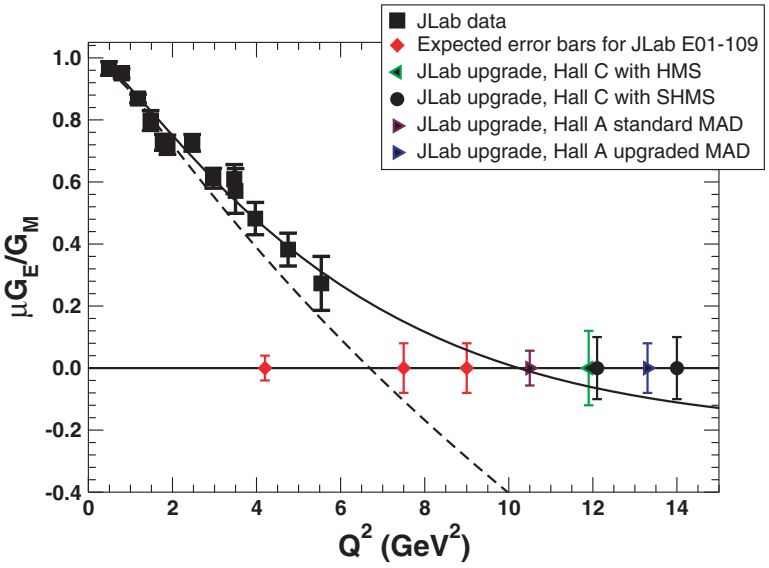

Figure 8: The result of the JLab measurement of G_E^p/G_M^p (black squares), and the range of the projected measurements. The dashed curve corresponds to the purely soft GPD of Burkardt [Bu02], and the solid curve results when an additional short range component is added. The difference between these two curves demonstrates how high Q^2 form factor data will constrain our knowledge of the short range behavior of the nucleon wave function.

the measurement of the four nucleon form factors to the highest possible Q^2 and to express all four in terms of common GPDs. Only the magnetic form factor of the proton, G_M^p, has been measured to high $Q^2(\sim 30\ (\mathrm{GeV}/c)^2)$ with relatively good accuracy. With the 12 GeV upgrade, G_E^p/G_M^p can be measured up to 14 $(\mathrm{GeV}/c)^2$. Knowledge of neutron form factors at high Q^2 is equally important. For the neutron, G_M^n would be extended up to about 14 $(\mathrm{GeV}/c)^2$, and for G_E^n to 5 $(\mathrm{GeV}/c)^2$.

Recent JLab results (Fig. 8) show the potential for discovery with increasing Q^2; before this experiment it was thought that G_E^p was roughly equal to G_M^p/μ. These data demonstrate that charge and magnetization distributions in the proton are quite different. It provides a challenge for theory to explain these results. By extending the Q^2 range of this data by over a factor of two, JLab at 12 GeV will probe the proton's structure to distances as small as 0.1 fm.

Real Compton Scattering (RCS) at high $|t|$ and wide angles involves the measurement of cross sections and longitudinal and transverse polarizations. In the GPD picture the observables involve the $\langle 1/x \rangle$ moments. The recent JLab data have been interpreted in this framework. The high $|t|$ behavior of the GPDs and therefore the transverse distribution of quarks at small impact parameters in the nucleon will be significantly constrained by extended RCS measurements. With the 12 GeV upgrade it will be possible to extend $|t|$ and s up to 20 $(\mathrm{GeV}/c)^2$. The RCS form factors R_V, R_T, and R_A are expected to scale with s and $|t|$ according to pQCD. The higher $|t|$ data could provide important information on this transition to pQCD, and an essential complement to Virtual Compton Scattering data.

Resonance transition form factors access additional GPD components that are not directly probed by elastic scattering or Real Compton Scattering. The form factors for the transition to the first excited state of the nucleon (the $N \to \Delta$ transition) are connected to the isovector components of the GPDs. With the 12 GeV upgrade the dominant $N \to \Delta$ form factor would be extended to almost 18 $(\mathrm{GeV}/c)^2$. Similarly, the multipole ratio E_{1+}/M_{1+}, which at small $|t|$ is related to the deformation of the nucleon and the Δ, would be extended up to about 12 $(\mathrm{GeV}/c)^2$. One might see the ratio depart from its current near zero value to approach the pQCD prediction that $E_{1+}/M_{1+} = 1$ in this Q^2 range. The transition to $S_{11}(1535)$ will also be studied. The S_{11} amplitude is expected to scale with Q^3. Current data to $Q^2 = 4$ $(\mathrm{GeV}/c)^2$ do not yet show the expected scaling behavior. The upgraded facility would allow extensions of the data up to about 20 $(\mathrm{GeV}/c)^2$.

Valence Quark Structure and Parton Distributions The 12 GeV Upgrade will allow us to map out the quark distribution functions with high precision in the "clean" high-x region where the three basic ("valence") quarks of dominate the proton and neutron wavefunction. Such measurements will have a profound impact on our understanding of the structure of the proton and neutron. They will also provide essential inputs for calculating hard cross sections at high energy hadron colliders such as the LHC or the Tevatron, in searches for the Higgs boson or for physics beyond the Standard Model.

Figure 9 shows an example of a measurement that can be done with the proposed Upgrade. The neutron polarization asymmetry A_1^n is determined by the spin wavefunction of the quarks, and most dynamical models predict that in the limit where a single valence up or down quark carries all of the nucleon's momentum ($x \to 1$), it will also carry all of the spin polarization (so, *e.g.* for the neutron, $A_1^n \to 1$ as $x \to 1$). Existing data on A_1^n end before reaching the region of valence quark dominance, and show no sign of making the predicted dramatic transition $A_1^n \to 1$ (the recent data from the Hall A experiment E99-117 show the first hint of a possible upturn at the largest x value). There are similar paucities of data on all other DIS observables in this region.

Figures 10 and 11 show two more examples of the power of the 12 GeV upgrade for the study of valence quark structure (in both cases focused on d-quark structure). For the down quarks in the proton even the sign of the polarization at large x is not known (see Fig. 10). The polarization of individual quark flavors can be determined by detecting final state hadrons (such as pions or kaons) in coincidence with the scattered electron. These "semi-inclusive" deep inelastic scattering experiments will, in addition, allow us to study the "sea" quarks belonging to the quark-antiquark pairs at lower x, independently of the valence quarks. They will also provide access to new, hitherto unmeasured distributions such as the "transversity", which describes the distribution of transversely polarized quarks in a transversely polarized nucleon.

Even in unpolarized DIS, where the available data are best, there are unresolved issues. To extract the ratio of such a simple and basic a property as the relative probability of finding a d quark vs. a u quark at high x requires measurements on both the proton and neutron. However, high-x

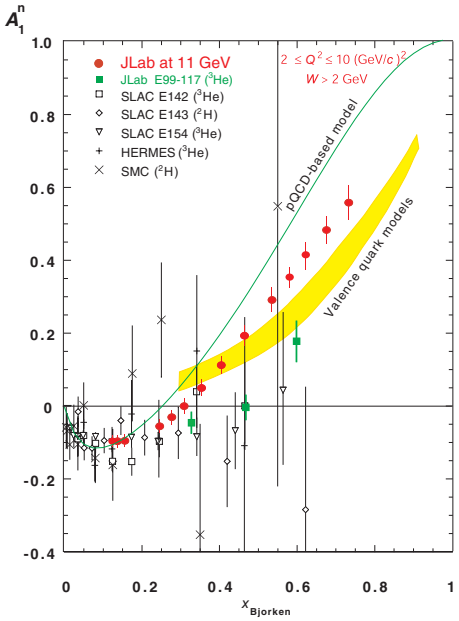

Figure 9: A projected measurement of the neutron polarization asymmetry A_1^n, determined by the spin structure of the valence quarks, made possible by the proposed 12 GeV Upgrade. The shaded band represents the range of predictions of valence quark models; the solid line is the prediction of a perturbative QCD (pQCD)-based quark model.

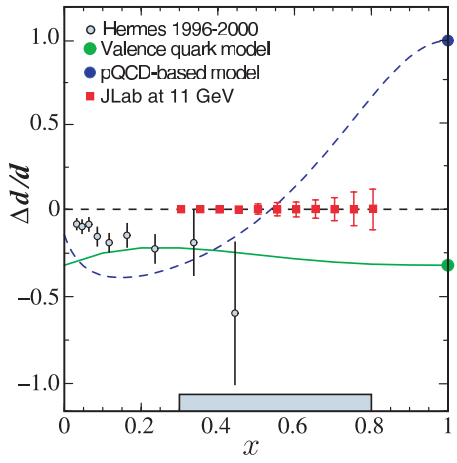

Figure 10: The ratio of polarized to unpolarized valence down quark distribution functions measured in semi-inclusive deep inelastic scattering. The solid squares represent the predicted accuracy with a 12 GeV Upgrade, with the systematic error indicated by the blue band. The solid (green) curve uses wavefunctions from a valence quark model, while the dashed (blue) uses pQCD-constrained fits to the world data set.

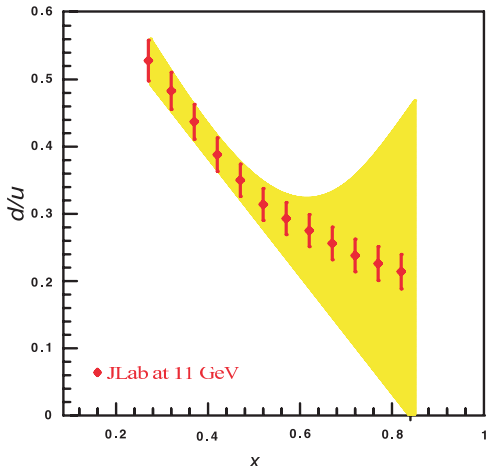

Figure 11: A projected measurement of the ratio of momentum distributions of valence d quarks to u quarks made possible by the proposed 12 GeV Upgrade. The shaded band represents the uncertainty in existing experiments due to nuclear Fermi motion effects.

neutron information is difficult to disentangle from nuclear binding corrections due to the deuterium target. Figure 11 shows the precision with which this fundamental ratio (which is intimately related to the fact that the proton and neutron, and not the Δ, are the stable building blocks of nuclei) can be measured with the proposed Upgrade. The proposed experiment will utilize a novel technique, currently being pioneered at JLab; a recoil proton detector "tags" scattering events on a nearly on-shell neutron in a deuteron target. The mirror symmetry of $A = 3$ nuclei could be exploited through simultaneous measurements of the inclusive structure functions for ^{3}He and ^{3}H to provide an independent measurement of this ratio. Both methods are designed to largely eliminate the nuclear corrections, thereby permitting the neutron-to-proton ratio (and thus the d/u ratio) to be extracted with unprecedented precision.

The measurement of structure functions over the large kinematic range made available with the 12 GeV Upgrade will also allow moments, or x-weighted integrals, of both spin-polarized and unpolarized structure functions to be determined accurately. Certain moments of polarized structure functions, for example, are related to the color-electric and magnetic polarizabilities of the nucleon, which characterize the response of the gluon fields to the nucleon's polarization. These moments are also directly calculable from first principles using lattice QCD simulations, and will thus provide critical tests of QCD itself.

The Generalized Parton Distributions as Accessed via Deeply Exclusive Reactions The Generalized Parton Distributions tell us a great deal more about the physics of partons than do the individual Feynman distributions and the form factors. For example, one can determine the quark angular momentum distribution from the GPDs. The total quark contribution to the spin of the nucleon can be determined by the following sum rule [Ji97]:

$$J^q = \frac{1}{2}\Delta\Sigma - L^q = \frac{1}{2}\int_{-1}^{1} x dx [H^q(x,\xi,0) + E^q(x,\xi,0)] \quad (1)$$

The quark spin part contribution, $\Delta\Sigma$, has been measured for the last decade through polarized deep-inelastic scattering. Therefore, an experimental determination of J^q allows a measurement of the quark orbital angular momentum, a quantity hard to determine otherwise.

One of the striking findings that has emerged from the theoretical study of the GPDs is that they can be measured through a new class of "hard" exclusive processes: Deeply Virtual Compton Scattering (DVCS) and Deeply Virtual Meson Production (DVMP). Both of these reactions are a subset of deep inelastic scattering in which specific exclusive final states are measured. As shown schematically in Fig. 12, in DVCS the electron knocks a quark out of the proton by exchanging a deeply virtual (massive) photon. The quark then emits a high energy photon and is put back into the proton, emitting a photon. In DVMP a $q\bar{q}$ pair is created, and a quark is returned into the proton while the $\bar{q}$ picks up a quark from the vacuum to form a meson. At sufficiently high energy and virtuality of the exchanged photon (Bjorken regime) these hard processes can be described by perturbative QCD, and the cross sections can be used to extract the "soft" information of the nucleon described by the GPDs.

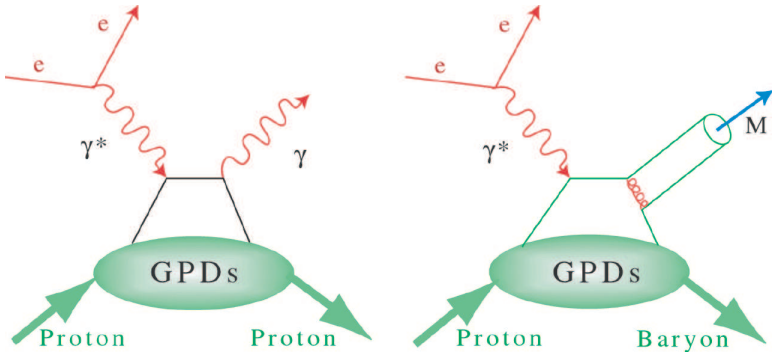

Figure 12: The "handbag" diagrams for deeply virtual Compton scattering (left), and for deeply virtual meson production (right). Four GPDs describe the "soft" proton structure part. They depend on the longitudinal quark momentum fraction x, and two more variables: the longitudinal momentum imbalance of the quark before and after the interaction, ξ, and the momentum transfered to the proton, t.

At energies and momentum transfers currently available at JLab, photons are produced not only via DVCS but also (even more copiously) via the electromagnetic Bethe-Heitler (BH) process. The two processes interfere, and the BH term, which is completely determined by the well known elastic form factors, "boosts" the much smaller and unknown DVCS term, which is determined by the GPDs, to comfortably measurable levels. During the past two years DVCS has become an established tool of GPD studies with experimental results from CLAS [St01] at JLab and from the HERA experiments H1 [Ad01], ZEUS [Sa01], and HERMES [Ai01]. These data are well described in a consistent GPD analysis in leading order (LO) and next to leading order (NLO) QCD [Fr01], supporting the applicability of the GPD formalism to exclusive photon production even at relatively low Q^2. An example of the broad kinematic coverage in Q^2, x_B, and t for the DVCS program, achievable with the equipment proposed for the 12 GeV upgrade, is shown in Fig.13. Similar coverage can be achieved for the GPD program in meson production.

Polarized beam asymmetry measurements allow the extraction of GPDs or linear combinations of GPDs at fixed kinematics $x = \xi$, while cross section measurements determine integrals of GPDs at fixed values of ξ and t. Different combinations of GPDs can be measured using polarized targets. DVCS off unpolarized protons cannot separate contributions from different quark flavors or separate the spin-dependent from the spin-independent GPDs. DVMP is another tool to study GPDs; it can make these separations. Vector meson production, (*e.g.* ρ and ω) permit the isolation of the spin-independent GPDs and separate u and d quark contributions, while pseudoscalar meson production (*e.g.* π^0, η) accesses the spin-dependent GPDs.

A full program to extract GPDs from measurements requires coverage of a large kinematic range in ξ, t, and Q^2, and measurement of several final states together with the use of polarized beam and polarized targets with longitudinal and transverse polarization. The 12 GeV upgrade of the electron accelerator and of the equipment required for the GPD program will provide the kinematic coverage needed for a broad program of DVCS and DVMP. Doubling the energy of the

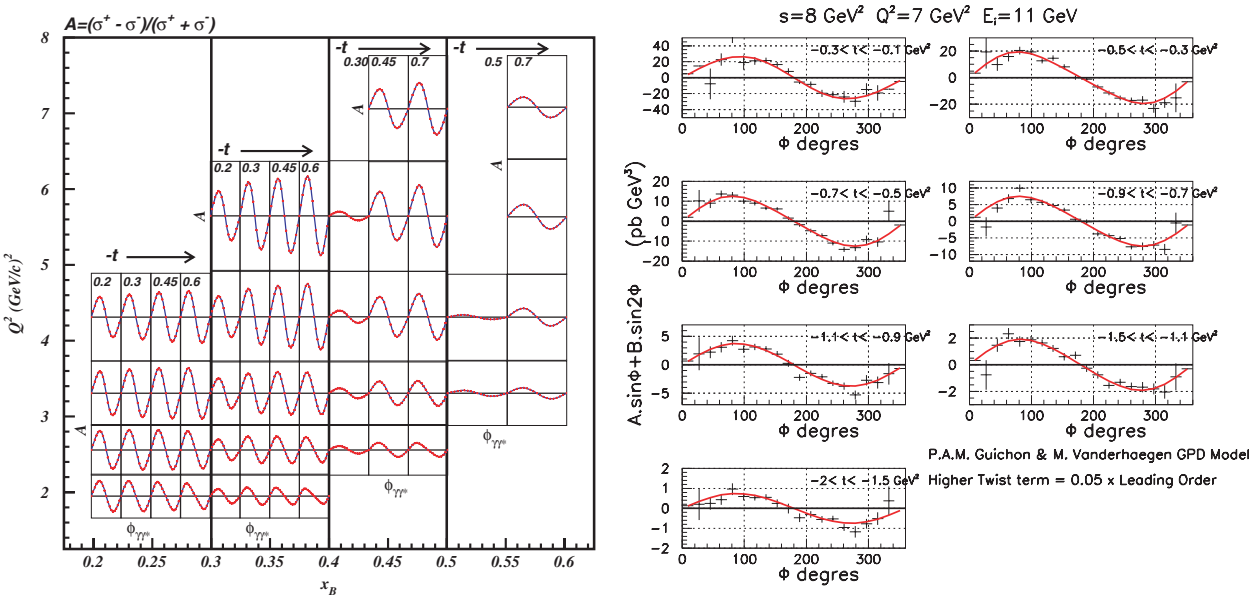

Figure 13: Beam spin asymmetry for $\vec{e}p \to ep\gamma$. Projected data and error bars for kinematic coverage of DVCS/BH asymmetry measurements. The left panel shows the lower t portion of azimuthal asymmetries that can be accessed simultaneously. The curves represent a specific model for the GPDs. The right panel shows projected data at the highest Q^2 for cross section differences. In kinematics, where the DVCS cross section is large, absolute cross section measurements will be possible giving access to moments of different combinations of GPDs.

current accelerator in conjunction with the very high luminosity will allow access to the highest Q^2 and ξ values of any facility worldwide. These unprecedented capabilities will allow a comprehensive program of DVCS and DVMP to be carried out.

The results of this program, together with results at smaller ξ from other laboratories, will form the basis for the ultimate extraction of the GPDs, and will strongly constrain the modeling of quark flavor and spin distributions in the transverse plane [Bu02]. Figure 14 shows a distribution for the u and d quarks in unpolarized and in transversely polarized protons, as constructed from models for the GPD $H(x, \xi = 0, b_\perp)$ and $E(x, \xi = 0, b_\perp)$, giving a visualization of the proton's quark-flavor distribution and the spin-flavor polarization emerging in a transversely polarized proton. Even five years ago it was unimaginable that we would ever be able to obtain such detailed and revealing images of proton structure.

Other Topics in Hadron Structure In addition to the broadly focused programs described above, the 12 GeV Upgrade will support important research directions into other aspects of hadron structure. Two examples presented here are the use of semi-inclusive scattering to access quark transverse momentum effects, and the study of duality – the emergence of the nucleon as an object in its own right from its quark-gluon substructure.

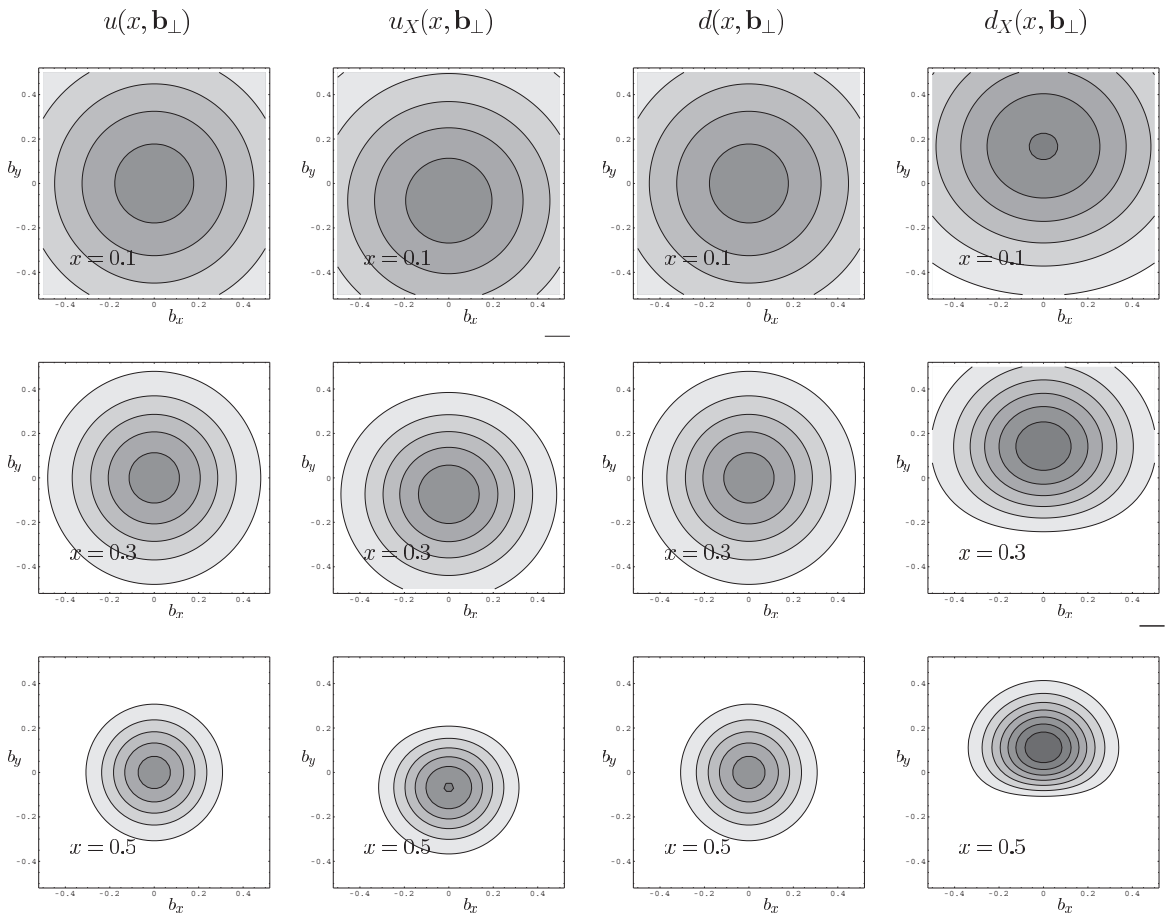

Figure 14: The quark spatial and spin distributions in the transverse plane from model calculations. The left panels show the u quark longitudinal momentum and helicity distributions in transverse impact parameter space. The panels on the right show the corresponding images for the d quarks in the proton. A strong correlation between the transverse size and the longitudinal momentum is evident. For small quark momentum fractions x, the proton has a large transverse size, and it becomes very dense at large x. The right columns in each panel show the quark spin distributions in a transversely polarized proton. u and d quarks exhibit a strong and opposite spatial asymmetry. Quarks in a transversely polarized protons have a strong spin-flavor polarization, especially at high x. The general features of these plots are model independent.

Transverse parton distributions The transverse momentum dependent (TMD) parton distributions [Ra88, Mu96] are a class of functions that represent information on the transverse hadron structure; they are complementary to the GPDs and encode information on the orbital motion of quarks. Experimentally, TMDs can be accessed in measurements of azimuthal distributions of final state photons or hadrons in semi-inclusive deep inelastic scattering, From this quark transverse momentum distributions can be obtained. A theoretical understanding of this new information is now emerging. It has been shown [Co93, Br02] that initial and final state interactions at the parton level are probed. TMDs also provide a new avenue for probing the chiral nature of the partonic structure of hadrons [Co02]. Single spin asymmetries are sensitive to this information even at lower energies [Ba02, Be01]. The first experimental data show significant asymmetries using polarized targets (HERMES at DESY), (SMC at CERN), and polarized beams (CLAS at JLab). Already at the 4-6 GeV energies at JLab, the data are consistent with a partonic interpretation. At the 12 GeV Upgrade the single spin asymmetries with polarized beams and polarized targets could become another pillar in the study of the quark spatial and spin distribution in the transverse momentum plane, with the ultimate goal of unraveling the new parton physics encoded in the GPDs and TMDs, especially in the effort to understand the orbital motion of quarks.

The extended GDH integral and sum rule The extended GDH integral[Ji01, Dr00], $I(Q^2)$, can be measured from arbitrarily small Q^2, where behavior is dominated by hadronic degrees of freedom, to arbitrarily large Q^2, where behavior is dominated by quark degrees of freedom[Am02]. A weighted integral over the difference of the spin-dependent total cross sections for virtual photoabsorption, $I(Q^2)$ is firmly tied theoretically by the GDH sum rule at $Q^2 = 0$ [Ge66, Dr66], and by both experimental and theoretical constraints as $Q^2 \to \infty$. As such, it is an excellent proving ground for quantitative tests of our understanding of the transition from perturbative to non-perturbative regimes. Accurate determinations of $I(Q^2)$, however, require measurements over a wide range of Q^2 at energies corresponding to both the resonance region as well as deep inelastic scattering. At 6 GeV, measurements are confined largely to the resonance region. With the 12 GeV upgrade, studies of the extended GDH sum rule will have the kinematic coverage necessary to probe the high-energy piece of the extended GDH integral. The program will compliment real-photon studies planned at SLAC, and bring GDH studies to a new level of quantitative precision.

Duality: the transition from a hadronic to a quark-gluon description of Deep Inelastic Scattering For many years, particle and nuclear physicists have noticed a striking similarity between data measured at extremely high energies, where electrons scatter from quarks in relative isolation, and data at lower energies, where electrons scatter from a proton that responds coherently. This observed similarity is known as quark-hadron duality. This quark-hadron duality at low energy naturally examines the transition between strongly interacting matter and the quark-gluon descriptions of perturbative QCD. Recently, there has been significant progress in quantifying and understanding duality. To further understand the phenomena underlying duality, however,

studies with different flavor and spin filters (including L/T separations) are needed with the much wider range of kinematics accessible with 11 GeV electrons. For structure functions where duality is demonstrably valid, parton distribution functions can be extracted at higher x than possible if traditional limits defining the quark-gluon regime are imposed. Duality studies are also crucial in establishing kinematics where fragmentation can be applied in the interpretation of semi-inclusive scattering experiments.

1.A.3 The Physics of Nuclei

A great deal of nuclear properties and reactions over a wide energy range – from the few keV regime of astrophysical relevance to the MeV regime of nuclear spectra to the tens to hundreds of MeV regime measured in nuclear response experiments – can be understood quantitatively by describing nuclei as assemblies of individual nucleons bound by effective interactions.

The dominant two-body interaction has a component at large internucleon distances (≥ 2 fm) due to pion exchange, which is theoretically well understood. The main feature of this one-pion-exchange component is its tensor character, which leads to a strong coupling between the nucleons' spatial and spin degrees of freedom. These spin-space correlations make nuclei markedly different from other systems where the dominant interaction is independent of the particles' internal degrees of freedom (spin and isospin), such as the Coulomb interaction in atoms and molecules and the van der Waals interaction in liquid Helium.

At short internucleon distances, the two-body interaction is thought to be influenced by heavy-meson and quark-exchange mechanisms, and by the excitation of nucleon resonances. It is poorly understood, although it is well constrained phenomenologically (at least below the pion production threshold) by the large body of pp and np elastic scattering data. It is predominantly characterized by a strong repulsion.

The interplay between these two aspects of the nucleon-nucleon interaction–its short-range repulsion and long-range tensor character–have profound consequences for the spatial and spin structure of nuclei [Fo96]. For example, the deuteron, the simplest nucleus consisting of a proton and neutron bound together, has a toroidal shape when the proton's and neutron's spins are opposite, and a dumbbell shape when their spins are aligned. This picture of the deuteron has been confirmed experimentally, in its broad outlines, by the recent measurement of the tensor polarization of the deuteron in elastic eD scattering at Jefferson Lab.

These short-range and tensor correlations are reflected in many nuclear properties. For example, the density distributions in nuclei of two-nucleon states with deuteron-like quantum numbers are very small at small internucleon separations and exhibit strong anisotropies depending on the relative orientation of the two nucleons's spins; in the region $r \leq 2$ fm, they are found to differ from those in the deuteron only by an overall scale factor depending on the mass number of

the nucleus [Fo96]. Another example of the impact of correlations is the increase in the relative probability of finding, within the nucleus, a nucleon with a very high momentum.

The $N-N$ interaction at large distances is well-represented by pion exchange; at short and intermediate distances, meson-exchange mechanisms (with phenomenologically determined couplings and short-range cutoffs) provide a good representation that leads naturally to effective many-body currents. There is a great deal of experimental evidence for the presence of these meson-exchange currents in nuclei from measurements of the charge and magnetic form factors of the hydrogen and helium isotopes, deuteron electrodisintegration at threshold, and low-energy radiative capture reactions involving few-nucleon systems.

While the description of nuclei outlined above provides a coherent and deceptively simple framework for the understanding of their properties over the range of energy and momentum transfers measured so far, it leaves unanswered several crucial questions:

- How do these effective interactions involving nucleons and mesons arise from the underlying dynamics of quarks and gluons ?
- Down to what distance scale does the short-range structure of nuclei implied by these interactions remain valid ?
- How does the transition from the nucleon-meson- to the quark-gluon-based description of nuclei occur and what are its signatures ?

Answers to these questions, taken together with an understanding of the QCD basis for the structure of the hadrons (the focus of the second major research thrust of the Upgrade, as outlined in Section 1.A.2 above) will provide an intellectually firm foundation for our understanding of nuclear physics that is analogous to our understanding of the physics of atoms, molecules and condensed matter based on the underlying theory of quantum electrodynamics.

The Short-Range Behavior of the $N-N$ Interaction and Its QCD Basis The 12 GeV Upgrade will provide unique opportunities for an understanding of how the $N-N$ interaction emerges from the underlying quark-gluon structure of the individual nucleons, identifying of the responsible mechanisms through, for example, studies of the phenomenon of color transparency in exclusive processes, color van der Waals-type interactions in ψ-meson photoproduction, and quark propagation and hadronization in the nuclear medium. The details of the short range behavior of the $N-N$ force will also be explored by a novel program of deep inelastic scattering aimed toward identifying the heretofore elusive (to experiment) short range correlations among the nucleons. Relevant experimental programs are outlined below, and described in detail in Chapter 2. Much of the information gained from these experiments will also be useful in completing our understanding of the transition from the meson/nucleon description of nuclei to the underlying quark and gluon description – the second major program in the physics of the nucleus, which is outlined below.

Color transparency. The nature of hadronic interactions can be investigated via tests of the prediction of "color transparency". Color transparency is one of the few direct manifestations of the underlying color degrees-of-freedom in nuclear physics. Under the right conditions, three quarks, each of which (alone) would have interacted very strongly with nuclear matter, could form an object that passes undisturbed through the nuclear medium. A similar phenomenon occurs in QED, where an e^+e^- pair of small size has a small cross section determined by its electric dipole moment. In QCD, a $q\bar{q}$ or qqq system with a small color dipole moment is predicted to have similarly reduced interactions due to cancelation of the color fields of the quarks. While the $q\bar{q}$ case is completely analogous to the QED example given, color transparency in the qqq case would be one of the rare demonstrations of the $SU(3)$ nature of the underlying color degrees of freedom. While the nucleonic example is more exotic, meson production may provide a more practical setting for observing this phenomenon. Intuitively, one expects an earlier onset of color transparency for meson production, as it is much more probable to produce a small sized configuration in a $q\bar{q}$ system than in the qqq system. Color transparency can be observed experimentally by measuring a reduced attenuation of particles as they exit a nucleus, or by measuring a decrease in production of particles produced via two-step rescattering mechanisms, which allows the use of few-body nuclei. A series of attenuation and rescattering measurements for both protons and mesons will allow us to separate the necessary ingredients: formation of the small sized configuration, the reduced color interaction of these configurations, and the evolution of these exotic configurations back into ordinary hadrons. The observation of color transparency and characterization of the non-perturbative evolution of a mini-hadron to its physical size will lead to a better understanding of the dynamics of confinement.

Learning about the NN force by the measurement of the threshold ψN cross section and by searching for ψ-nucleus bound states. Threshold ψ photoproduction is a unique process since the small $c\bar{c}$ state is produced by the interaction of its calculable small color dipole moment with a nucleon (in which it is presumed to *induce* a large, but uncalculable, color dipole moment). This simple color van der Waals–type force is a prototype for a potentially important component of the NN force. It is quite possible that this interaction is sufficiently strong that ψN or ψ-nucleus bound states exist. Such relatively long-lived objects might be detected in subthreshold ψ production off nuclei. Based on the same picture, one could also look for ϕN states. Each exchanged gluon may also couple to a colored cluster and reveal the hidden color part of the nuclear wave function, as well as multiquark correlations, a domain of short range nuclear physics at high density where nucleons lose their identity. Finally the formation time of the ψ, much shorter than the size of the nucleus, gives access to a more reliable determination of the $\psi - N$ scattering cross section, an important input in the search of the signature of quark-gluon plasma. Only the high intensity and duty factor of the beams available from an upgraded CEBAF make it possible to exploit the potential of discovery of such an almost virgin field.

Quark propagation through cold QCD matter: nuclear hadronization and transverse momentum broadening. The properties of isolated quarks are generally experimentally inaccessible due to quark confinement in hadrons. In hard interactions, such as in deep inelastic scattering, the struck quark in a nucleon must separate from the rest of the residual system. When this separation distance is comparable to nuclear radii, it is possible to study the properties of the propagating quark by varying the radii of the nuclear targets and observing modifications of the final hadronic states. The distances over which the struck quark transforms into a new hadron can be characterized as a function of multiple variables. This provides completely new information on how the color field of the hadron is restored in real time through the fundamental process of gluon emission. The analogous process has been studied and understood in QED. The propagating quark is expected to experience some interaction with the nuclear medium. One prediction is that it undergoes multiple soft scatterings mediated by gluon emission. In this picture, the quark experiences a medium-induced energy loss that may be experimentally accessible and which may exhibit exotic coherence phenomena. This process measurably broadens the transverse momentum distribution of the hadron emerging from larger nuclei. It is anticipated that a quark-gluon correlation function, and the quark energy loss, can be extracted from the measured broadening. The topics of color field restoration by gluon emission, quark-gluon correlations, and quark energy loss, offer fundamental and interesting insights into the nature of QCD and confinement. In addition, they are of very high interest in the study of relativistic A-A and p-A collisions, where they are basic and essential ingredients that must be understood.

Short-range correlations in nuclei: the nature of QCD at high density and the structure of cold, dense nuclear matter. The upgrade will allow substantial extensions to JLab's studies of high-momentum components of nuclear wavefunctions and short-range nucleon-nucleon correlations. With a variety of measurements made in the three existing halls, the upgrade will answer several questions about nuclear many-body theory and map out the strength and nature of two-nucleon and multi-nucleon correlations in nuclei. These short-range correlations represent high density droplets of nuclear matter with instantaneous densities comparable to those at which the zero temperature quark-gluon phase transition is expected to occur (Fig. 15). The structure of nucleons and the distribution of high-momentum quarks may be substantially altered in this region, where significant overlap of nucleons should allow direct interaction between quarks in different nucleons. These measurements will allow us to determine if such modification of nucleon structure is responsible for the EMC effect, and will help us understand the quark-gluon phase transition at high density. This complements RHIC studies of this same transition at high temperature, while at the same time providing us information on the structure of matter at extremely high densities. Probing these high density components in nuclei is the only way to directly study high density nuclear matter, and what we learn here will be important in understanding neutron stars and other compact astronomical objects.

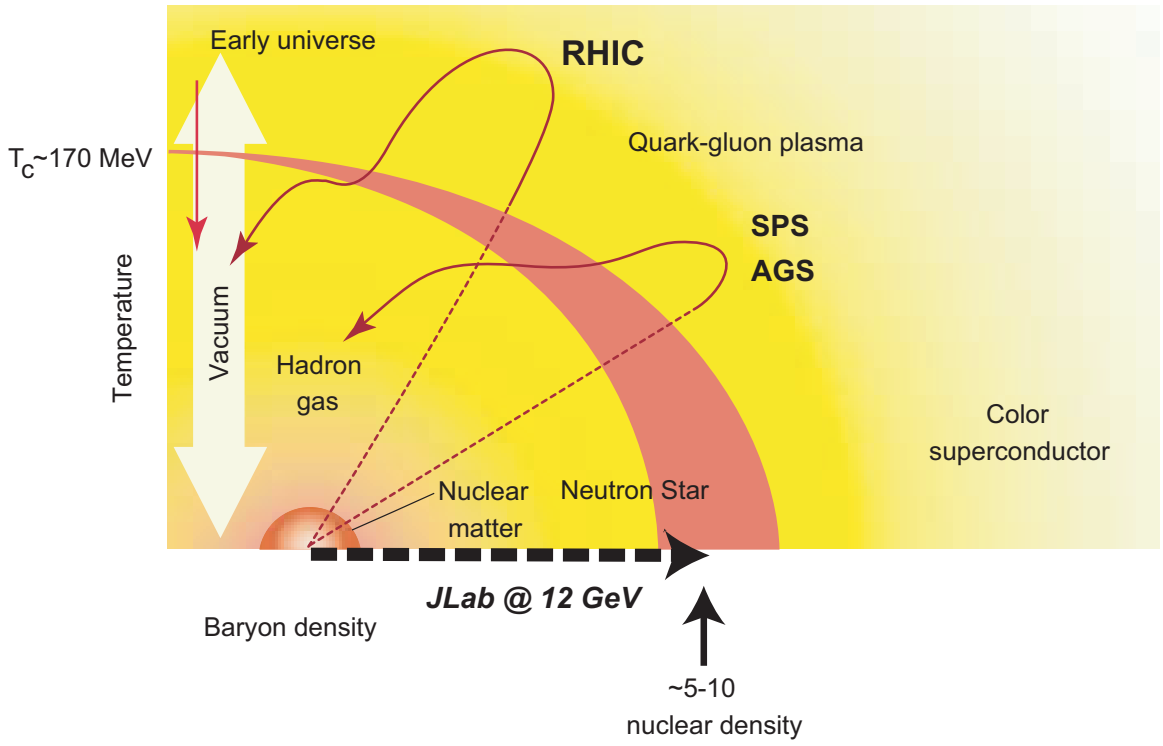

Figure 15: Phase diagram for nuclear matter. With the energy upgrade, JLab will be able to probe cold nuclear matter at extremely high density. The red band indicates the phase transition from hadronic to quark matter.

Identifying and Exploring the Transition from the Meson/Nucleon Description of Nuclei to the Underlying Quark and Gluon Description. The hadron to parton transition region is another interesting and important open question in nuclear physics. Low energy nuclear physics has been described successfully using effective interactions among nucleons, *i.e.* in terms of hadronic degrees of freedom. On the other hand, at sufficiently high energy, perturbative QCD (pQCD) describes hadronic reactions in terms of quark and gluon degrees of freedom. Very little is known about the transition between these two regimes, in particular there are no clear indications from theory as to the energy range in which it should occur; it must be mapped out by experiment.

An important search for this elusive transition region can be carried out with the 12-GeV upgrade envisioned for Jefferson Lab. The strategy outlined below is to search for it in the simplest systems, *i.e.* in the pion and nucleon, since these are the hadronic building blocks of nuclei at low energy, and in the deuteron and Helium isotopes, since these nuclei are particularly amenable to theoretical interpretation. Some proposed signals for the transition region are observation of scaling and hadron helicity conservation (in addition to other possible signals, such as color transparency, which is described above). The proposed high-current 12-GeV electron beam coupled with relatively large acceptance detectors will be essential tools in searching for these exotic effects. Relevant experimental programs are outlined below, and described in detail in Chapter 2. Much of the information gained from these experiments will also be useful in developing an understanding of the short range behavior of the $N-N$ interaction and how it emerges from the underlying quark-gluon structure of the individual nucleons.

The onset of scaling behavior in nuclear cross sections Scaling in the differential cross section $d\sigma/dt$, and hadron helicity conservation have been pursued experimentally for many years as providing signatures of the transition from the meson/nucleon description of nuclei to the underlying quark and gluon description. The deuteron photodisintegration reaction, $\gamma d \to pn$, is one of the simplest reactions for studying explicit quark effects in nuclei. In recent years, extensive studies of deuteron photo-disintegration have been carried out at SLAC and JLab [Na88, Sc01]. Figure 16 shows the scaled differential cross-section ($s^{11}d\sigma/dt$) for deuteron photodisintegration as a function of photon energy. The available data [Sc01] seem to show scaling at 70° and 90°, and suggest the onset of scaling at higher photon energies at 52° and 36°. The threshold for this scaling behavior corresponds to a transverse momentum slightly over 1 GeV. Theoretical efforts [Fr01, Ko93, Gr01, Rapc] to describe this behavior agree qualitatively with the data, but do not reproduce them precisely. While none of the theories agree with all of the data as well as one would like, they do indicate that quark models can approximately reproduce the cross section data, and therefore re-establish the importance of the deuteron photodisintegration process in the study of the transition region. The Upgrade will permit the extension of these data to photon energies near 8 GeV, as shown in the figure, permitting a confirmation of the apparent constant transverse momentum onset of scaling behavior.

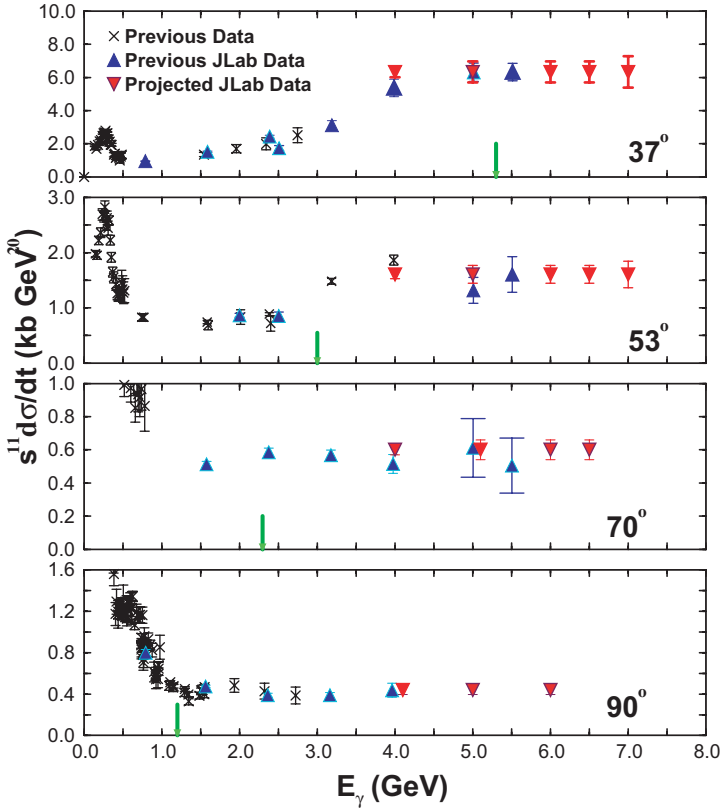

Figure 16: Available data projected results for a differential cross-section measurement of deuteron photodisintegration.

Helicity conservation in nuclear reactions While global scaling behavior has been observed in many exclusive processes [An76], no experimental evidence supports hadron helicity conservation, which was predicted in the same approach, in the similar energy and momentum transfer region. The hadron helicity conservation arises from the vector coupling nature of the quark-gluon interaction, the quark helicity conservation at high energies, and the neglect of the non-zero quark orbital angular momentum state in the nucleon. The parton orbital angular momentum was considered for the first time by Chernyak and Zhitnitsky [Ch77a] for form factors. Recently, Ji, Ma, and Yuan [Ji03] derived a generalized counting rule for exclusive processes at fixed angles involving parton orbital angular momentum and hadron helicity flip. This generalized counting rule opens a new window for probing the quark orbital angular momentum state inside the nucleon by employing exclusive processes. A natural connection between the study of the parton-hadron transition through exclusive processes and generalized parton distributions typically probed through deeply virtual processes is therefore established.

Polarization measurements can play a crucial role in understanding reaction mechanisms of exclusive processes at large momentum transfers. Therefore, they are important measurements in the transition region that will provide insights into the underlying mechanism governing the onset of the scaling behavior and test the hadron helicity conservation rule. Furthermore, the combination of precise differential cross-section and polarization measurements allows unique access to the parton orbital angular momentum inside the nucleon based on the newly-derived generalized counting rule [Ji03]. The upgrade would permit the extension of polarization data from deuteron photo-disintegration [Kr01] to ~ 4 GeV, and from $\vec{\gamma}p \to \vec{p}\pi^0$ reaction to approximately 8 GeV.

The charged pion form factor To complete our understanding of 'strong' QCD one essential piece of information is an understanding of when the dynamics of the strong interaction makes a transition from being dominated by the strong QCD [Cl95a] of confinement to perturbative QCD. This transition should occur first in the simplest systems; in particular, the pion elastic form factor seems the best hope for seeing this transition experimentally because of its simple $q\bar{q}$ valence quark structure. Figure 17 shows available data on the pion form factor, and how well the proposed 12 GeV Upgrade can explore this transition.

Pion photoproduction off the nucleon and in the nuclear medium Due to its simplicity, the pion form factor provides our best hope for direct comparison with rigorous QCD calculations. As can be seen from Fig. 17, it is still dominated by non-perturbative effects at a few $(\mathrm{GeV/c})^2$. An earlier onset to the scaling associated with pQCD may be seen by forming ratios of cross sections. The simplest of such ratios is the charged pion photoproduction differential cross-section ratio, $\frac{d\sigma}{dt}(\gamma n \to \pi^- p)/\frac{d\sigma}{dt}(\gamma p \to \pi^+ n)$. Although no factorization theorem exists for the transverse pion photoproduction process, it is thought to be dominated by a one-hard gluon exchange process at high energies. In such a ratio, non-perturbative effects are predicted to cancel and one may expect the π^-/π^+ ratio to give the first indication of the onset of pQCD [Hu00]. The

charged pion ratio has been measured at Jefferson Lab for momentum transfers up to 5.0 $(\mathrm{GeV/c})^2$. This ratio measurement can be extended to a $|t|$ value of about 10 $(\mathrm{GeV/c})^2$, significantly higher than the projected Q^2 value of 6.0 $(\mathrm{GeV/c})^2$ for the charged pion form factor measurement with a 11 GeV beam. Figure 18 shows both the available data and projected results for this ratio at 11 GeV, together with a prediction of Huang and Kroll [Hu00].

Nucleon photopion production processes are also essential probes of the hadron/parton transition region. Because they decrease relatively slowly with energy compared to other photon-induced processes (quark counting rules predict a s^{-7}-dependence for the differential cross-section), the cross sections of these processes are advantageous for the investigation of an observed oscillatory QCD scaling behavior. This behavior is thought to arise from the interference of the hard pQCD (short-distance) amplitude and the long-distance (Landshoff) amplitude; it is analogous to the QED effect of Coulomb-nuclear interference observed in low energy charged particle scattering. The relatively higher rates for these processes will allow investigations of the t and p_T dependence of scaling behavior and the study of the s dependence. Recent results from deuteron photo-disintegration [Sc01] show for the first time an angular dependent onset for the scaling behavior in photoreactions and p_T seems to be the physical observable governing the onset of the scaling behavior. Therefore, it is essential to carry out similar studies in other photon induced exclusive processes. Photopion production from nuclei also allows the search for novel pQCD effects such as nuclear filtering and color transparency.

1.A.4 Symmetry Tests in Nuclear Physics

Precision parity-violating electron scattering experiments made feasible by the 12 GeV Upgrade have the sensitivity to search for deviations from the Standard Model that could signal the presence of new gauge bosons Z's, the existence of leptoquarks, or particles predicted by supersymmetric theories, *i.e.* physics beyond the Standard Model. Planned studies of the three neutral pseudoscalar mesons, the π^0, η and η', will provide fundamental information about low energy QCD, including certain critical low energy parameters, the effects of SU(3) and isospin breaking by the u, d, and s quark masses, and the strengths of the two types of chiral anomalies. These two programs are described briefly below, and in detail in Chapter 2.

Standard Model Tests Precision electro-weak measurements are potentially sensitive to physics beyond the Standard Model even below the energies needed to produce new particles directly. At the same time, they can provide new insights into novel aspects of hadron structure. For these reasons, the ongoing JLab program of Standard Model tests using parity violating electron scattering, exemplified by the approved weak proton charge experiment, will be extended to 12 GeV with exciting new opportunities.

Of clear importance will be an improved measurement of the weak charge of the electron. In

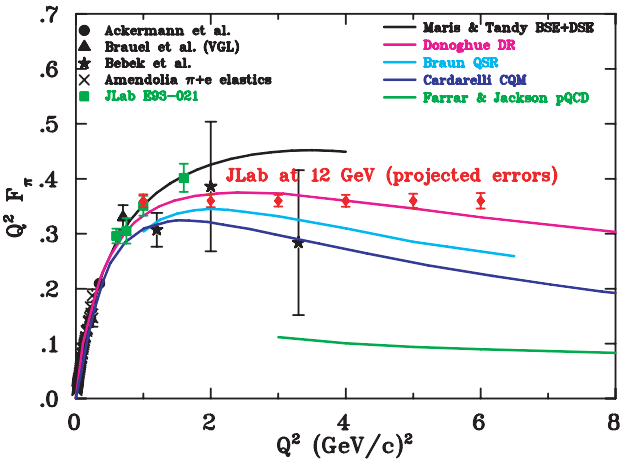

Figure 17: The projected measurements of the pion elastic form factor through the expected transition region from confinement-dominated dynamics to perturbative-dominated dynamics made possible by the proposed 12 GeV Upgrade. Also shown are a few of the dozens of model predictions, all characterized by being confinement-dominated below about 2 $(\mathrm{GeV}/c)^2$ and making a transition to being perturbative-dominated with a value of $Q^2 F_\pi \simeq 0.1$ $(\mathrm{GeV}/c)^2$ in the region of 10 $(\mathrm{GeV}/c)^2$.

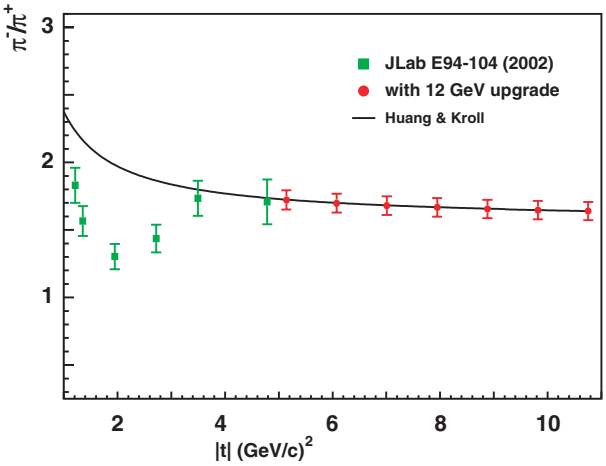

Figure 18: The charged pion photoproduction differential cross-section ratio at a C.M. angle of 90°, as a function of $|t|$ $(\mathrm{GeV/c})^2$ (blue) along with the projected measurements for JLab at 11 GeV (red). The solid curve is a prediction by Huang and Kroll [Hu00].

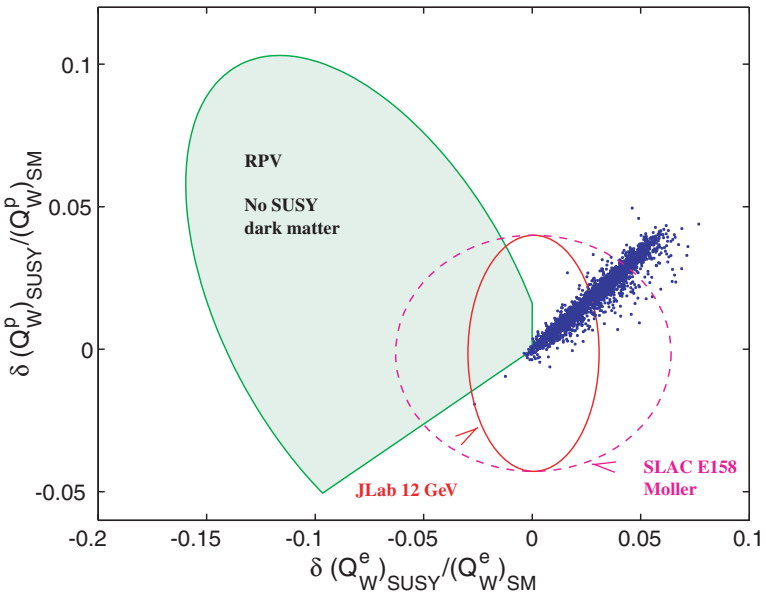

Figure 19: Relative shifts in $Q^e_{\rm weak}$ and $Q^{\rm proton}_{\rm weak}$ from SUSY effects. The blue dots indicate MSSM loop corrections for approximately 3000 SUSY-breaking parameter choices. The interior of the green truncated ellipse shows possible shifts due to R-parity violation. In this region, SUSY dark matter is excluded [Ku02]. The dashed magenta ellipse illustrates the expected uncertainty from SLAC E-158 Møller and JLab Q-Weak, while the red ellipse represents what could be achieved with a 12 GeV Møller experiment at Jefferson Laboratory.

principle, an uncertainty which is half that of the anticipated SLAC E158 error can be achieved. A measurement with this precision would be a powerful tool in the search for "new physics", and even a result in agreement with the Standard Model would have significant consequences. For example, such a result would severely constrain the viability of SUSY models that lack a candidate particle for dark matter, the non-luminous and unexplained source of 90% of the mass of the universe (see Fig. 19). However, a precision measurement of such a small asymmetry (40 ppb) will require extraordinary control of systematic errors and 200 days of running time.

By contrast, parity violation in deep inelastic scattering (DIS) is characterized by relatively large asymmetries and, hence, potentially short running times. The measurement of this reaction by Prescott *et al.* established the Standard Model as the correct theory of the neutral weak interaction. A recent study of neutrino-nucleus DIS by the NuTeV collaboration suggests that the Standard Model description of this interaction is incomplete. An 11 GeV measurement of parity violating DIS could help determine whether the NuTeV "anomaly" is an artifact of poorly understood hadronic physics or a true indication of new physics. It could also provide a new window on higher-twist structure functions.

Properties of Light Pseudoscalar Mesons via the Primakoff Effect Two basic phenomena in QCD, namely the spontaneous breaking of chiral symmetry and the chiral anomalies, are mani-

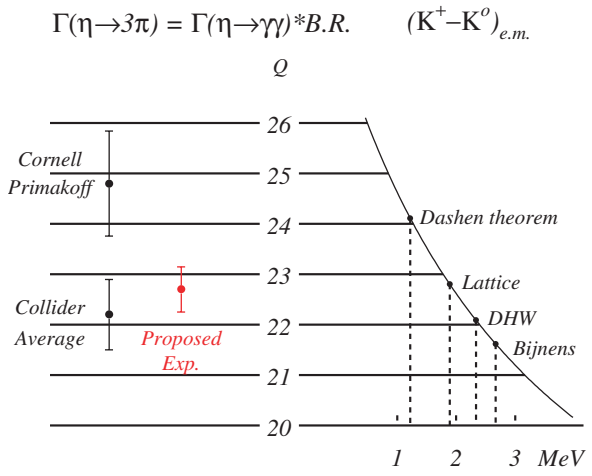

Figure 20: The importance of $\Gamma_{\eta\to\gamma\gamma}$ in the measurement of the quark mass ratio $\mathcal{Q}$, where $\mathcal{Q}^2 = \frac{m_s^2-\hat{m}^2}{m_d^2-m_u^2}$ and $\hat{m} = (m_u + m_d)/2$. The *l.h.s.* indicates the values of $\mathcal{Q}$ corresponding to the Primakoff and collider experimental results for $\Gamma_{\eta\to\gamma\gamma}$, and the projected result for Jefferson Laboratory with 12 GeV. The *r.h.s.* shows the results for $\mathcal{Q}$ obtained with four different theoretical estimates of the electromagnetic self energies of the kaons. The figure is adapted from Leutwyler.

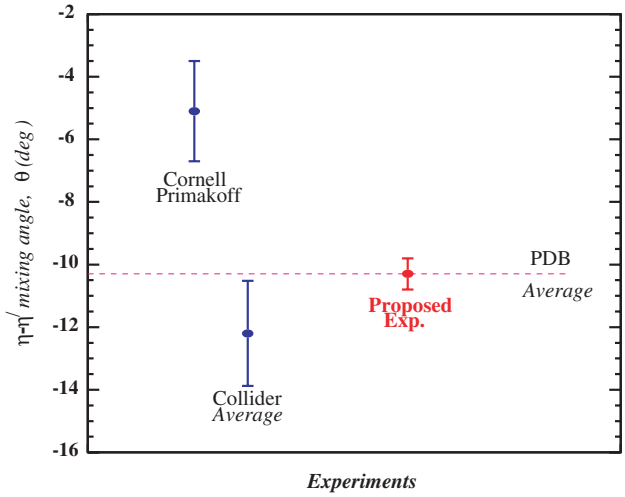

Figure 21: The $\eta-\eta'$ mixing angle as determined by a previous Primakoff measurement, $\gamma-\gamma$ collisions, and the projected result with the Jefferson Laboratory 12 GeV Upgrade

fested in their most unambiguous form in the sector of light pseudoscalar mesons. The anomalies particularly drive the two-photon decays of the π^o, η, and η' and also provide a large fraction of the η' mass. The effects of explicit chiral symmetry breaking by the non-vanishing u, d, and s quark masses also show through in the masses of these neutral pseudoscalars as well as in some of their decays. Indeed, important information about quark masses can be obtained from these mesons.

The advent of a 12 GeV electron beam at Jefferson Laboratory will make it possible to extend the current development of a high precision measurement of the $\pi^o \to \gamma\gamma$ decay width via the Primakoff effect to include the η and η' mesons. It will also enable a measurement of the transition form factors of these mesons. These measurements would have a significant impact on our knowledge of the ratios of quark masses, and particularly on ratios involving the differences in the masses of the u and d quarks. As indicated in Fig. 20, an important limitation on our knowledge of a ratio of the light quark masses is the experimental discrepancy between the η width determined by the $\gamma\gamma \to \eta$ reaction in e^+e^- collisions and that determined by a previous Primakoff experiment. An improved measurement of the Primakoff cross sections would significantly improve this situation.

More precise measurements of both the η and η' widths would provide stringent tests of both

QCD and QCD based models, particularly for the magnitude of $\eta - \eta^{'}$ mixing as shown in Fig. 21. At a more general level, these measurements impact the issue of whether the $\eta^{'}$ meson can be considered to be an approximate Goldstone Boson in the combined chiral and large N_c expansions. The proposed measurements of the π^o, η and η' transition form factors at very low Q^2 ($\sim$ 0.001–0.5 GeV^2) would provide a first measurement of these important quantities. The η' form factor slope specifically tests the U(3) flavor symmetry implied by the large N_c limit. In this limit, the same low energy constant in chiral perturbation theory determines all three transition form factor slopes.

The proposed instrumentation for this program involves an upgraded version of the photon detection system used in the π^0 lifetime experiment. This instrumentation will be of general utility for both this program and future experiments, and will provide a new and powerful experimental window on QCD at Jefferson Laboratory in an arena where the basic theory is well established. In addition, more precise knowledge of the transition form factors of the pseudoscalar mesons is required for a better determination of the so called light-by-light scattering contributions to the anomalous magnetic moment of the muon, which is one of the most sensitive quantities to new physics beyond the Standard Model.

1.B Upgrade Project Summary

While this Pre-Conceptual Design Report is focused on a description of the science driving the 12 GeV Upgrade, in order to provide a complete overview, this section gives a brief summary of the laboratory's plans for the accelerator, based on a 25 May 1999 internal JLab report, *Interim Point Design for the CEBAF 12 GeV Upgrade* and additional work that has been carried out to refine the design since that report was issued. It also outlines our plans for the new detector and detector upgrade projects necessary to carry out the program.

The key features of CEBAF that make the Upgrade so cost-effective are easily defined. By the summer of 1994, CEBAF had installed what was the world's largest superconducting radio-frequency (SRF) accelerator: an interconnected pair of antiparallel linacs, each comprising 20 cryomodules, with each cryomodule in turn containing eight SRF accelerating cavities. On average, these cavities exceed their design specifications by 50% in the two critical performance measures: accelerating gradient and Q. It is the success of this technology that has opened up the possibility of a relatively simple and inexpensive upgrade of CEBAF's top energy. This technological success would not be so readily multiplied if considerable foresight had not also been exercised in laying out the CEBAF tunnel "footprint", which was designed so that the magnetic arcs could accommodate an electron beam of up to 24 GeV. The latent accelerating power of the installed SRF cavities has already brought CEBAF to 6 GeV, 50% above its design energy, and recent successes in SRF development have led to the production of two cryomodules that are more than a factor of 2 more powerful than the original design. A staged development program is underway that is aimed at a

cryomodule that exceeds the original specification by a factor of 5 using higher-performing seven-cell cavities but fits into the same space as the original cryomodules based on five-cell cavities). The cryomodule developed as the first step in this program shows initial performance that is a factor of 4 better than the original specifications, consistent with the design goals. Using the space already available in the linac tunnels to install ten of the final-design cryomodules 12 GeV can be attained at a modest cost.

The equipment planned for the Upgrade project takes full advantage of apparatus developed for the present program. In each of the existing halls, new spectrometers are added and/or present equipment upgraded to meet the demands of the 12 GeV program. Then a new hall, Hall D, will be added to support the meson spectroscopy program.

In Hall A, the Upgrade will add a large angular- and momentum-acceptance, moderate-resolution magnetic spectrometer (to be called the Medium-Acceptance Device, or MAD) and a high-resolution electromagnetic calorimeter. The spectrometer will provide a tool for high-luminosity, high-x studies of the properties of nucleons with an 11 GeV beam, and will also be used for selected investigations of the GPD's, where high luminosity and good resolution are needed. Details are provided in Section 3.A of this document. In Hall B, the CEBAF Large Acceptance Spectrometer (CLAS), which was designed to study multi-particle, exclusive reactions with its combination of large acceptance and moderate momentum resolution, will be upgraded to CLAS^{++} and optimized for studying exclusive reactions (emphasizing the investigation of the GPD's) at high energy. It will also be used for selected valence quark structure studies involving neutron "tagging" or polarized targets capable of supporting only very low beam current. Most importantly, the maximum luminosity will be upgraded from 10^{34} to 10^{35} cm^{-2} s^{-1}. The present toroidal magnet, time-of-flight counters, Čerenkov detectors, and shower counter will be retained, but the tracking system and other details of the central region of the detector will be changed to match the new physics goals. Details are provided in Section 3.B. In Hall C a new, high-momentum spectrometer (the SHMS, Super-High-Momentum Spectrometer) will be constructed to support high-luminosity experiments detecting reaction products with momenta up to the full 11 GeV beam energy. This feature is essential for studies such as the pion form factor, color transparency, duality, and high-Q^2 N^* form factors. The spectrometer will be usable at very small scattering angles. See Section 3.C for details. Finally, in Hall D, a tagged coherent bremsstrahlung beam and solenoidal detector will be constructed in support of a program of gluonic spectroscopy aimed at testing experimentally our current understanding that quark confinement arises from the formation of QCD flux tubes. This apparatus is described in detail in Section 3.D.

1.B.1 The Accelerator

The accelerator portion of the Upgrade is straightforward. The basic elements can be seen in Fig. 22, and the key parameters of the upgraded accelerator are listed in Table 1. The Upgrade utilizes the existing tunnel and does not change the basic layout of the accelerator. There are four

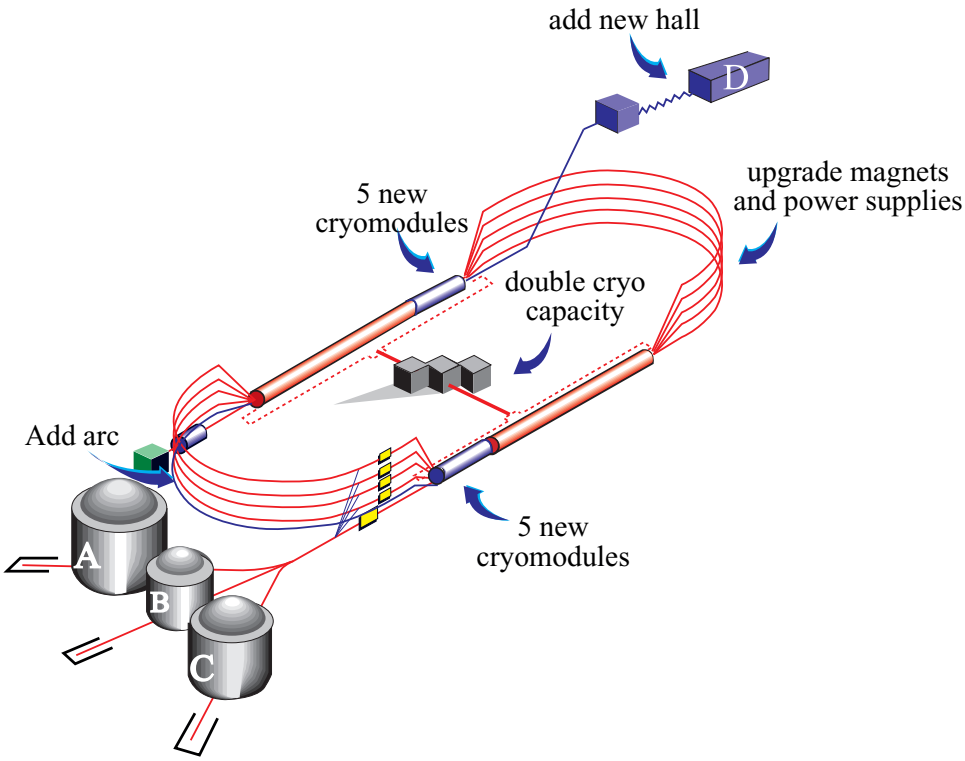

Figure 22: The configuration of the proposed 12 GeV CEBAF Upgrade.

Table 1: Selected key parameters of the CEBAF 12 GeV Upgrade

Parameter	Specification
Number of passes for Hall D	5.5 (add a tenth arc)
Max. energy to Hall D	12.1 GeV (for 9 GeV photons)
Number of passes for Halls A, B, C	5
Max. energy to Halls A, B, C	11.0 GeV
Max. energy gain per pass	2.2 GeV
Range of energy gain per pass	3:1
Duty factor	cw
Max. summed current to Halls A, C* (at full, 5-pass energy)	85 μA
Max. summed current to Halls B, D	5 μA
New cryomodules	10 (5 per linac)
Central Helium Liquifier upgrade	10.1 kW (from present 4.8 kW)

*Max. *total* beam power is 1 MW.

main changes: additional acceleration in the linacs, stronger magnets for the recirculation, an upgraded cryoplant, and the addition of a tenth recirculation arc. The extra arc permits an additional "half pass" through the accelerator to reach the required 12 GeV beam energy, followed by beam transport to Hall D that will be added to support the meson spectroscopy initiative.

Motivated by the science, the 12 GeV Upgrade derives its name from the fact that it will deliver a 12 GeV electron beam to the new end station, Hall D, where it will be used to produce 9 GeV polarized photons for the new gluonic and $s\bar{s}$ spectroscopies. The accelerator will, in addition, be able to simultaneously send electrons of 2.2, 4.4, 6.6, 8.8, or 11.0 GeV to the existing Halls A, B, and C. The increased physics power of the present halls comes from the qualitative jump in energy and momentum transfer that the Upgrade brings, and from the enhanced instrumentation capabilities planned for the detector complements in each of them. In describing the physics in Halls A, B, and C we will often refer to an 11 GeV electron beam (to be precise about the maximum beam energy available in these halls) but we will use the phrase "12 GeV" to describe the overall Upgrade.

1.B.2 The Experimental Equipment

Hall A and the Medium Acceptance Device (MAD) With the Jefferson Lab 12 GeV upgrade a large kinematics domain becomes accessible in deep inelastic scattering. The high luminosity and high polarization of beam and targets allow a unique contribution to the understanding of nucleon and nuclear structure, and the strong interaction in the high x region (which is dominated by the valence quarks). To fully utilize the high luminosity available at CEBAF (up to 10^{39} e $\cdot$ nucleons/cm^2/s), a well-matched spectrometer, given the name Medium-Acceptance Device (MAD), which can take this full luminosity while providing large angular and momentum acceptance, moderate momentum resolution, and good angular resolution, has been designed as the instrumental upgrade for Hall A. This spectrometer, which is shown in Fig. 23, will be used in conjunction with the existing HRS Spectrometers in Hall A.

The main elements of MAD are two warm-bore, combined-function (dipole and quadrupole) superconducting magnets. MAD has an angular acceptance of 28 msr for scattering angles $> 35^\circ$. Forward of 35° the distance between the target and the first quadrupole is increased, linearly decreasing the acceptance down to 6 msr at 12°. This acceptance remains available to scattering angles as forward as 6° through the use of a septum magnet. One of the existing HRS spectrometers will complement MAD, with an angular acceptance of up to 12 msr, an angular range between 6° - 150°, and a maximum momentum of 4.3 GeV/c. MAD can be oriented flexibly in order to accommodate the septum magnet while retaining a pointing accuracy ≤ 0.5 mrad as is required for accurate L/T separations. The design characteristics are summarized in Table 2.

A detector package has been designed for the detection of electrons and hadrons. The electron detection system will consist of four planes of scintillators for triggering, two drift chambers and one multi-wire proportional chamber for tracking and a gas Čerenkov counter and an electromagnetic

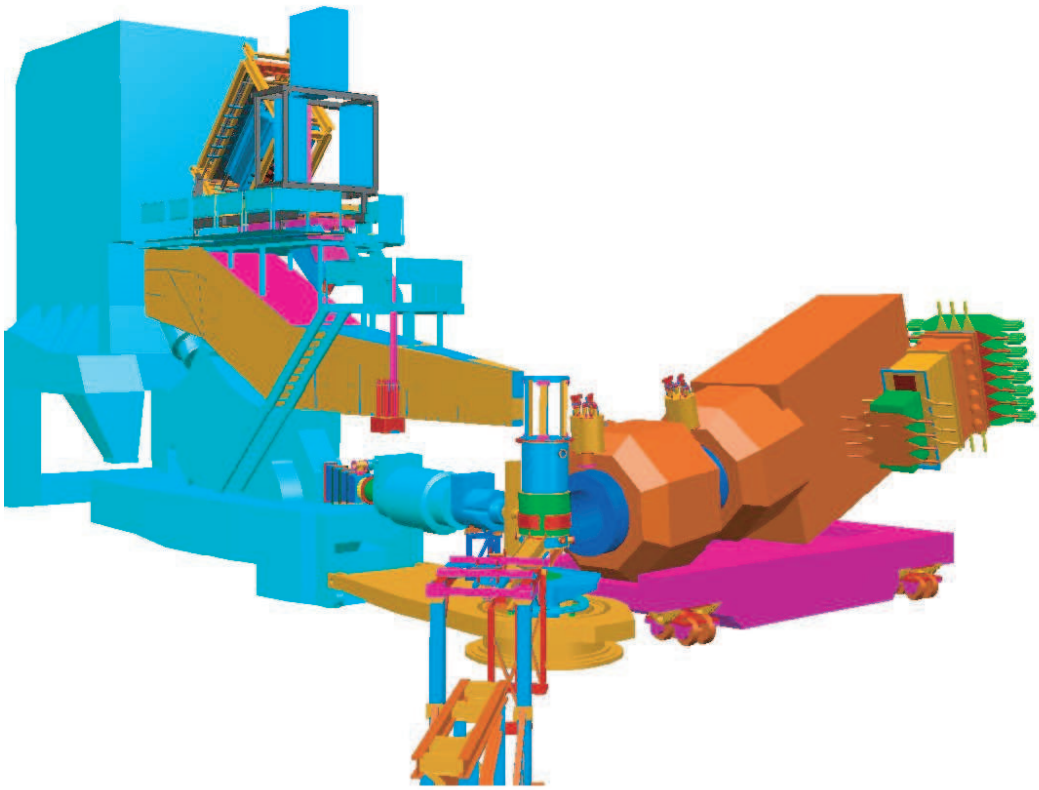

Figure 23: Three-dimensional CAD drawing of the MAD spectrometer

Table 2: The design characteristics of the MAD spectrometer shown along with HRS performance.

Parameter	MAD design	HRS performance
Central momentum range	0.4 - 6.0 GeV/c	0.2 - 4.3 GeV/c
Scattering angle range	6° - 130°	6° - 150°
Momentum acceptance	±15%	±5%
Momentum resolution	0.1%	0.02%
Angular acceptance	28 msr ($\geq$35°)	6 msr (standard)
	6 msr ($6° - 12°$)	12 msr (forward)
Angular resolution (hor)	1 mrad	0.5 mrad
Angular resolution (ver)	1 mrad	1 mrad
Target length acceptance (90°)	50 cm	10 cm
Vertex resolution	0.5 cm	0.1 cm
Maximum DAQ rate	20 kHz	5 kHz
e/h Discrimination	0.5×10^5 at 98%	2×10^5 at 99%
π/K Discrimination	100 at 95%	100 at 95%

calorimeter for particle-identification purposes. For hadron detection two aerogel Čerenkov counters and a focal plane polarimeter will be additionally available. Both packages provide excellent ($e^{\pm}, \pi^{\pm}, K^{\pm}$ and p) identification over the full momentum range. Pion rejection as good as a few times 10^{-5} will be provided. The data acquisition system is designed with a new generation of pipeline digitizing front-end electronics to be able to handle event rates up to 20 kHz.

In combination with the MAD spectrometer, a 100 msr lead-glass calorimeter is available for studies of nucleon form factors and of Real Compton Scattering. A large acceptance, high granularity calorimeter with 1296 element array of PbF_2 crystals is proposed to optimally study Generalized Parton Distributions through Deep Virtual Compton Scattering. It will also benefit other experiments, such as photo-production of neutral mesons at large transverse momenta.

In combination with the existing HRS in Hall A MAD will open up a window to a rich program of semi-inclusive experiments. The 12 GeV upgrade crosses the charm production threshold. Threshold charm production will benefit from MAD and the high luminosity. Precision experiments on nuclei at DIS conditions will become possible, and measurements of fundamental quantities (such as nucleon form factors) and novel QCD phenomena (such as color transparency) can be extended to higher Q^2. Because the cross sections drop rapidly with increasing Q^2, a high luminosity and a large acceptance spectrometer are crucial for precision measurements. Photoproduction at high energy provides a powerful tool to investigate the transition from the non-perturbative QCD region to the pQCD region. Again the rapidly falling cross section with increasing photon energy demands high luminosity and a large acceptance spectrometer. Precision data in this region will also have a significant impact on a search of new physics beyond the standard model at very high energies.

Hall B Upgrade and CLAS^{++}. The CLAS^{++} detector is shown in Fig. 24. It is designed to meet the basic requirements for the study of the Generalized Parton Distributions (GPDs) in deeply exclusive and semi-exclusive processes. CLAS^{++} also accommodates the requirements for measurements of polarized and unpolarized structure functions in inclusive processes. The main features of CLAS^{++} are:

- High operating luminosity of $10^{35}\text{cm}^{-2}\text{s}^{-1}$ for hydrogen targets, a ten-fold increase over current CLAS operating conditions.
- Improved detection capabilities for forward-going high momentum particles. Charged particles that bend outwards in the torus field can be reconstructed for angles as low as 5 degrees. Photon detection will be possible for angles as low as 3 degrees. Acceptance for electrons ranges from about 8 degrees to 40 degrees.
- Larger momentum range for the separation of electrons, pions, kaons, and protons. This is achieved with better resolution time-of-flight counters, and with the installation of a new threshold gas Čerenkov detector.

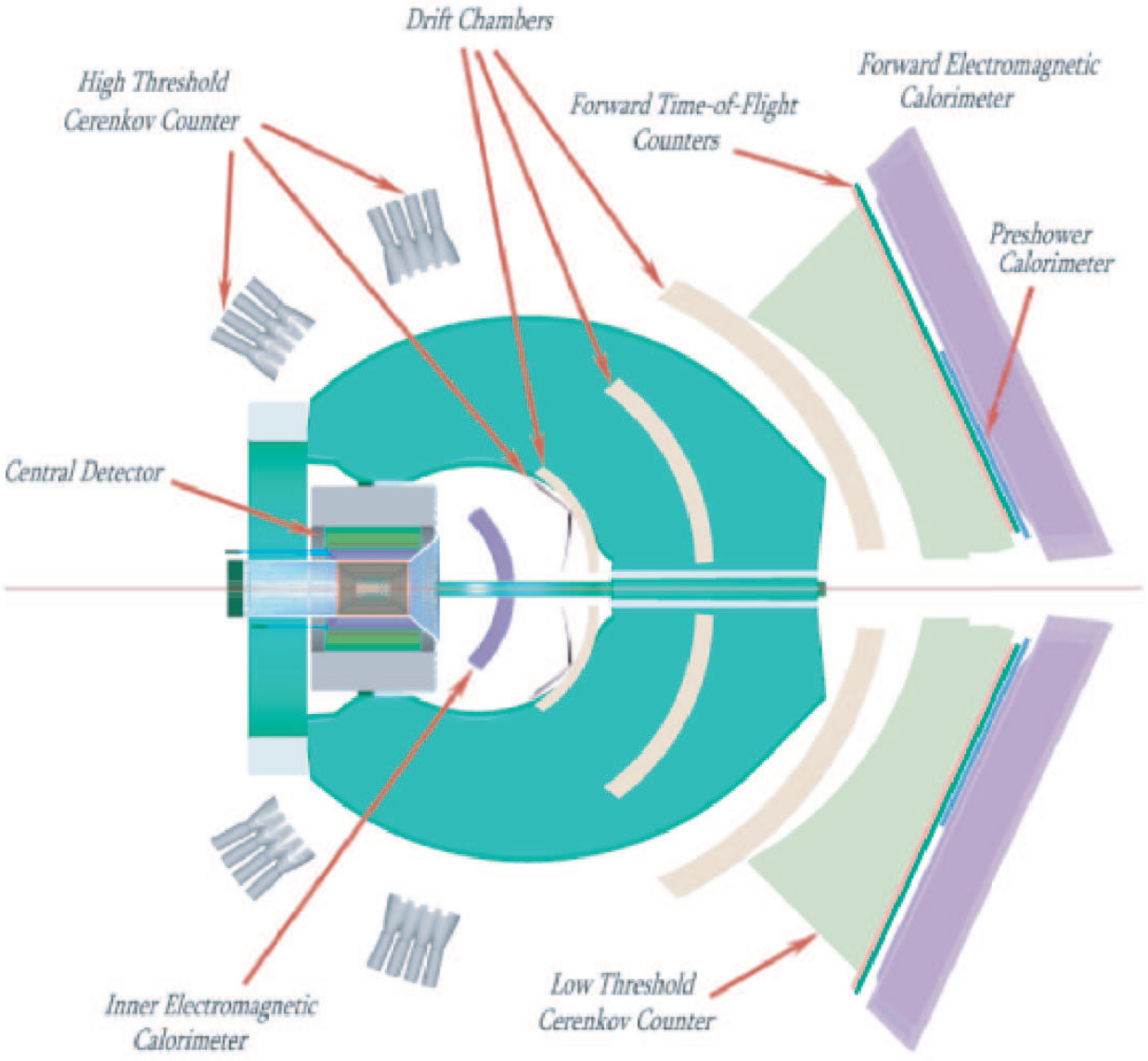

Figure 24: Section view of the CLAS^{++} detector.

- Capability to detect the recoiling baryons at large laboratory angles.

- Improved hermeticity for the detection of charged particles and photons in regions where CLAS currently has no detection capabilities, achieved by instrumenting the regions in front of the coils, and by extending the polar angle range for photon detection to 135 degrees.

- Capability to operate polarized solid state targets.

CLAS^{++} makes use of many of the components of the current CLAS detector, such as the Torus magnet, the forward electromagnetic calorimeters, Čerenkov detectors, and time-of-flight counters. Also, much of the drift chamber electronics will be reused. A new and essential component of CLAS^{++} is the Central Detector. Its main component is a superconducting solenoid magnet, which has a dual function: It replaces the existing mini-torus for shielding of the Møller electrons, and it provides the magnetic field for the momentum analysis of charged particles at large angles. Time-of-flight scintillators are used to provide particle identification at lab angles greater than 40 degrees. Due to the limited space available excellent timing resolution is essential. Tracking at large angles is provided by a combination of drift chambers with cathode strip readout and a microstrip detector near the vertex. Since most charged tracks will have momenta of 1.5 GeV/c or less, sufficient momentum resolution can be achieved even in the limited space available for tracking. A compact electromagnetic calorimeter based on tungsten powder and scintillating fiber technology provides photon detection capability for the angle range from 40-135 degrees.

Some modifications and additional detectors are needed in the Forward Detector as well. The main new component is a threshold gas Čerenkov counter for triggering on electrons. It will allow electron and pion separation up to nearly 5 GeV/c. Beyond 5 GeV/c, electrons are identified in the forward electromagnetic calorimeter. There is also additional electromagnetic calorimetry placed in front of the torus coils for improved hermiticity. Lead-tungstate crystals have emerged as a good choice for this detector.

A pre-shower detector will be inserted in front of the existing CLAS electromagnetic calorimeters. This detector will allow separation of single photons from $\pi^0 \to \gamma\gamma$ events; this is especially needed for deeply virtual Compton scattering. All drift chambers in CLAS will be replaced by new ones that will cover a smaller angle range with a factor of two smaller cell sizes to reduce the accidental hit occupancy due to photon interactions allowing for a corresponding gain in luminosity.

The existing forward detection system will be modified to extend particle identification and reconstruction to higher momenta. This will be accomplished by several means: The timing resolution of the scintillation counters will be improved by using smaller scintillator slabs, by adding an additional layer of scintillators, and by replacing the PMTs by new ones with better timing characteristics. This is expected to improve the timing resolution to about 60 psec. The existing gas Čerenkov counter will be modified slightly for improved pion detection capabilities for momenta greater than 2.7 GeV/c.

Tables 3 and 4 summarize the expected performance of CLAS^{++}. With these modifications and additions to the existing CLAS components, CLAS^{++} will be able to carry out the core program for the study of the internal nucleon dynamics and hadronization processes as listed here:

- Quark-gluon dynamics and nucleon tomography through measurement of deeply virtual Compton scattering and deeply virtual meson production, both with unpolarized and polarized hydrogen and deuterium targets.
- Polarized and unpolarized valence quark distributions at high x_B, using polarized hydrogen and deuterium targets, and by employing a novel technique of neutron tagging. Values of x_B up to 0.85 can be accessed in deep inelastic processes. A broad program of semi-inclusive measurements will allow quark-flavor tagging and give access to transverse quark structure functions.
- The magnetic structure of the neutron will be probed through magnetic form factor measurements up to 14 GeV^2, and the C2/M1 ratio for $N - \Delta(1232)$ up to $Q^2 = 12\ GeV^2$. Higher mass resonance transitions can be studied in multiple meson decays at high Q^2 as well.
- Space-time characteristics of quark hadronization and color transparency can be studied in nuclei in highly sensitive processes.
- Meson spectroscopy on ^4He, ^3He with a small angle quasi-real photon tagger, allows to eliminate baryonic background. Heavy baryon spectroscopy (e.g. Ξ^*) can be studied on hydrogen targets.

Hall C and the Super High Momentum Spectrometer (SHMS) At a 12-GeV Jefferson Lab, Hall C will provide a new magnetic spectrometer, the Super High Momentum Spectrometer (SHMS), powerful enough to analyze charged particles with momenta approaching that of the highest energy beam. Together with its companion, the existing High Momentum Spectrometer (HMS), this will make Hall C the only facility in the world capable of studying (deep) exclusive reactions up to the highest momentum transfers, $Q^2 \simeq 18$ (GeV/c)^2, with appropriate high luminosity. By extension, only Hall C will be able to fully exploit semi-exclusive reactions in the critical region where the electro-produced hadron carries almost all of the transfered energy .

Charged particles with such high momenta are boosted by relativistic kinematics into the forward detection hemisphere. Therefore, the SHMS is designed to achieve angles down to 5.5°, and up to 25°. The SHMS will cover a solid angle up to 4 msr, and boasts a large momentum and target acceptance. The existing HMS complements SHMS well, with a solid angle of up to 10 msr, an angular range between 10.5° and 90°, and a maximum momentum of 7.3 GeV/c.

Hall C's magnetic spectrometer pair will be rigidly connected to a central pivot that permits rapid, remote angle changes and reproducible rotation characteristics, which simplify accurate

Table 3: CLAS^{++}: acceptance and resolution

	Forward detector	Central Detector
Angular coverage		
Tracks (inbending)	$8^\circ - 37^\circ$	$40^\circ - 135^\circ$
Tracks (outbending)	$5^\circ - 37^\circ$	$40^\circ - 135^\circ$
Photons	$3^\circ - 37^\circ$	$40^\circ - 135^\circ$
Track resolution		
$\delta p/p$	$0.003 + 0.001p$	$\delta p_T/p_T = 0.02$
$\delta\theta(mr)$	1	8
$\delta\phi(mr)$	2-5	2
Photon detection		
Energy range (MeV)	> 150	> 60
$\delta\theta$ (mr)	4 (1 GeV)	15 (1 GeV)
Neutron detection		
η_{eff}	0.5 ($p > 1.5\ GeV/c$)	NA
Particle id		
Electron/pion	> 1000 ($p <$ 4.8GeV/c)	NA
	> 100 ($p >$ 4.8GeV/c	NA
π^+/π^-	full range	<0.65 GeV/c
K/π	full range	<0.65 GeV/c
$K^+/p, K^-/\bar{p}$	<4.5 GeV/c	<0.90 GeV/c
$\pi^\circ \to \gamma\gamma$	full range	full range
$\eta \to \gamma\gamma$	full range	full range

Table 4: CLAS^{++}: operating luminosity

Target	Luminosity ($10^{34} cm^{-2} s^{-1}$)
H_2	10
^3He	15
^2H, ^4He, ^{12}C, ^{16}O,..,Pb	20
NH_3, ND_3 (long. polarization)	20
NH_3, ND_3 (trans. polarization)	2

measurements such as Rosenbluth-type separations. From its inception, the SHMS momentum and target acceptances were designed to be large and nearly uniform, allowing for both fast and accurate data collection. The SHMS could operate at a luminosity of 10^{39} cm^{-2}s^{-1}, with a 40% momentum acceptance.

The large momentum acceptance, in combination with the large luminosity, will enable the measurement of the smallest cross sections, and allow for a complete map of the nucleon's response all the way from elastic scattering through deep inelastic scattering. The latter will greatly facilitate studies in the transition region from hadronic to quark-gluon degrees-of-freedom, including a novel determination of the spin and flavor dependence of low-energy quark-hadron duality and hadronization. The final product of these experiments will be a precise determination of the lowest moments of both spin- and flavor-dependent quark distributions for $Q^2 \leq 10$ (GeV/c)^2, providing a direct connection with Lattice QCD calculations.

Hall C will also retain its general infrastructure to offer collaborations an opportunity to do one-of-a-kind experiments, with dedicated experimental setups. Already at 6 GeV, the experimental program in Hall C will provide for 2 kW cryogenic target running, the use of an ≈100 msr electromagnetic calorimeter, and a focal-plane polarimeter suited for both HMS and SHMS operation at 12 GeV.

The overall specifications for the Hall C spectrometer setup for 12-GeV running are summarized in Table 5. Figure 25 shows the HMS and SHMS in both their most forward and most backward laboratory angle configurations.

With the new equipment, Hall C will be able to deliver, amongst others:

- Nucleon elastic and transition form factors up to $Q^2 \simeq 18$ (GeV/c)^2,
- Real Compton Scattering up to $s \simeq 20$ GeV^2,
- Deep exclusive pion and kaon electroproduction up to $Q^2 \simeq 10$ (GeV/c)^2, including precise longitudinal-transverse separations and spin-dependent measurements.
- A charged pion form factor measurement up to $Q^2 = 6$ (GeV/c)^2.
- Complete separation of the F_L, F_T, g_1, and g_2 inclusive structure functions of the proton (in the valence quark region) up to $Q^2 \simeq 10$ (GeV/c)^2.
- Precision measurements of the Q^2-dependence of nuclear effects in both inclusive structure functions and (deep) exclusive scattering, crossing the charm threshold.
- A parity-violating deep inelastic scattering experiment with unprecedented precision, to search for extensions of the Standard Model.

Table 5: Summary of the HMS performance and the design specifications for the SHMS.

Parameter	***HMS Performance***	***SHMS Specification***
Range of Central Momentum	0.4 to 7.3 GeV/c	2.5 to 11 GeV/c
Momentum Acceptance	$\pm$10%	-15% to +25%
Momentum Resolution	0.1% – 0.15%	$<$ 0.2%
Scattering Angle Range	10.5 to 90 degrees	5.5 to 25 degrees
Target Length Accepted at 90°	10 cm	50 cm
Horizontal Angle Acceptance	$\pm$32 mrad	$\pm$18 mrad
Vertical Angle Acceptance	$\pm$85 mrad	$\pm$50 mrad
Solid Angle Acceptance	8.1 msr	4 msr (LSA tune) 2 msr (SSA tune)
Horizontal Angle Resolution (yptar)	0.8 mrad	2-4 mrad
Vertical Angle Resolution (xptar)	1.0 mrad	1-2 mrad
Vertex Reconstruction Resolution (ytar)	0.3 cm	0.2 - 0.6 cm
Maximum DAQ Event Rate	2,000 events/second	10,000 events/second
Maximum Flux within Acceptance	$\sim$ 5 MHz	$\sim$ 5 MHz
e/h Discrimination	$>$1000:1 at 98% efficiency	1000:1 at 98% efficiency
π/K Discrimination	100:1 at 95% efficiency	100:1 at 95% efficiency

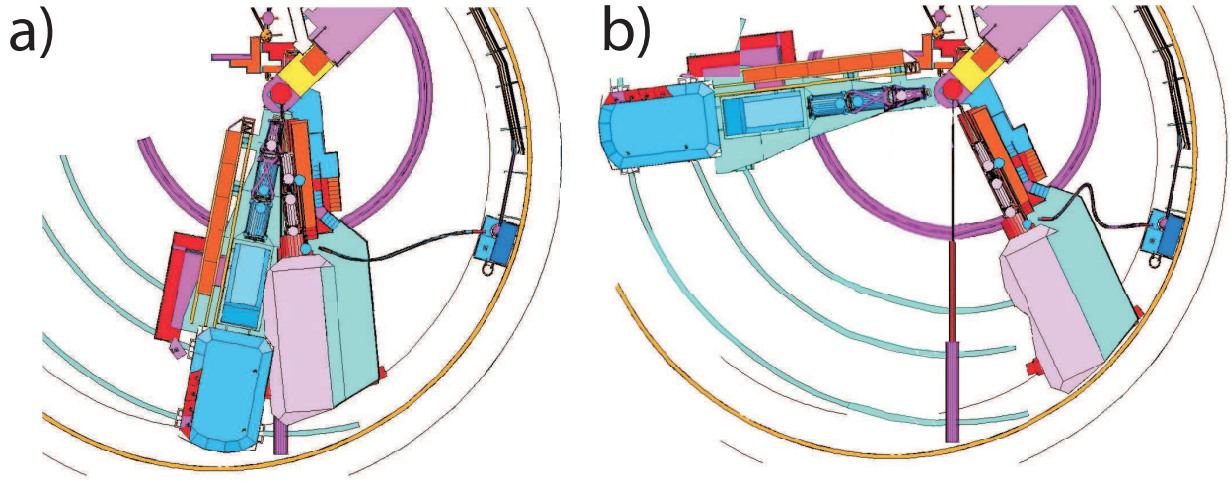

Figure 25: The SHMS-HMS spectrometer pair in two extreme configurations: a)the SHMS at 5.5° and the HMS at 10.5° ; and b) the SHMS at 25° and HMS at 85°.

Hall D and the GlueX Experiment The GlueX experiment will be housed in a new above-ground experimental hall (Hall D) located at the east end of the CEBAF north linac. A collimated beam of linearly polarized photons (with 40% polarization) of energy 8 to 9 GeV will be produced via coherent bremsstrahlung with 12 GeV electrons. This requires thin diamond crystal radiators (no more than 20 μ thick). The scattered electron from the bremsstrahlung will be tagged with sufficient precision to know the photon energy to within 0.1%.

The GlueX detector (see Fig. 26) uses an existing 2.25 T superconducting solenoid that is now being refurbished. An existing 3000-element lead-glass electromagnetic calorimeter will be reconfigured to match the downstream aperture of the solenoid. A threshold Čerenkov counter followed by a scintillator time-of-flight (TOF) wall will be placed between the solenoid and lead glass detector. Inside the full length of the solenoid a lead and scintillating fiber electromagnetic calorimeter will provide position and energy measurement for photons and TOF information for charged particles. A scintillating fiber vertex detector will surround the 30-cm long liquid hydrogen target. A cylindrical drift chambers will fill the region between the vertex detector and cylindrical calorimeter. Planar drift chambers will also be placed inside the solenoid downstream of the target.

This detector configuration has 4π hermeticity and momentum/energy and position information for charged particles and photons optimized for partial wave analysis. Extensive Monte Carlo studies for a wide variety of final states were carried out to certify the design parameters and the suitability of the detector for carrying out the final analysis.

An active program of R&D has been underway now for at least three years on each of the subsystems. Rocking curve measurements of diamond wafers have been carried out in the UK, and the coherent bremsstrahlung technique has been successfully demonstrated in Hall B. Prototypes of tracking elements and the cylindrical calorimeter have been built and more are planned. Beam tests in Russia on TOF prototypes have resulted in a finalized design. Prototype flash ADCs have been built and tested as have TDCs based on F1 chips. Work on optimizing electronics continues. More beam tests are planned. The magnet refurbishment project at the Indiana University Cyclotron Facility includes a plan to place detector elements inside the magnet and test them with an energized magnet.

The primary characteristics of the detector are given in Table 6. The hermetic design for the detector makes it an ideal tool to

- determine the masses and quantum numbers of mesons in the mass range of 1.5 to 2.5 GeV
- study properties of hybrid mesons produced at rates as low as a percent of normal mesons
- map out the poorly known spectra of $s\overline{s}$ mesons

The collaboration has carried out a partial wave analysis using simulated GlueX data. They are continuing to develop the collaboration, software and analysis tools needed to carry out partial

Table 6: Summary of the GlueX detector's characteristics.

Capability	***Quantity***	***Range***
Charged particles	Coverage	$1 \leq \theta \leq 170^\circ$
	Momentum resolution ($5 \leq \theta \leq 140^\circ$)	$\sigma_p/p \approx$ 1-2%
	Position resolution	$\sigma \approx$ 150-200μm
	dE/dx measurements	$20 \leq \theta \leq 140^\circ$
	Vertex detector	$\sigma \approx 500\mu$m
	Time-of-flight scintillators	$\sigma_t \approx 50$ ps
	Čerenkov for π/K separation	$\theta \leq 14^\circ$
	Barrel time resolution	$\sigma_t \approx 250$ ps
Photon detection	Energy measurements	$1 \leq \theta \leq 120^\circ$
	Veto capability	$\theta \geq 120^\circ$
	Lead glass energy resolution ($E_\gamma \geq 150$ MeV)	$\sigma_E/E \approx 2 + 5\%/\sqrt{E}$
	Barrel energy resolution ($E_\gamma \geq 20$ MeV)	$\sigma_E/E \approx 4.4\%/\sqrt{E}$
	Barrel position resolution	$\sigma_z \approx 1$ cm
DAQ / trigger	Level 1	200 KHz
	Event Rate	15 KHz to tape
	Data Rate	100 MB/s
Electronics	fully pipeline	Flash ADCs, TDCs
Photon Flux	Tagged rate	$10^8\gamma$/s

wave analysis on petabyte-size data sets starting with several tens of terabyte data sets (from other experiments) in hand. The collaboration is also developing experience in operating computer clusters at several different sites and plans to implement GRID tools and technologies which are deemed necessary to for the experiment.

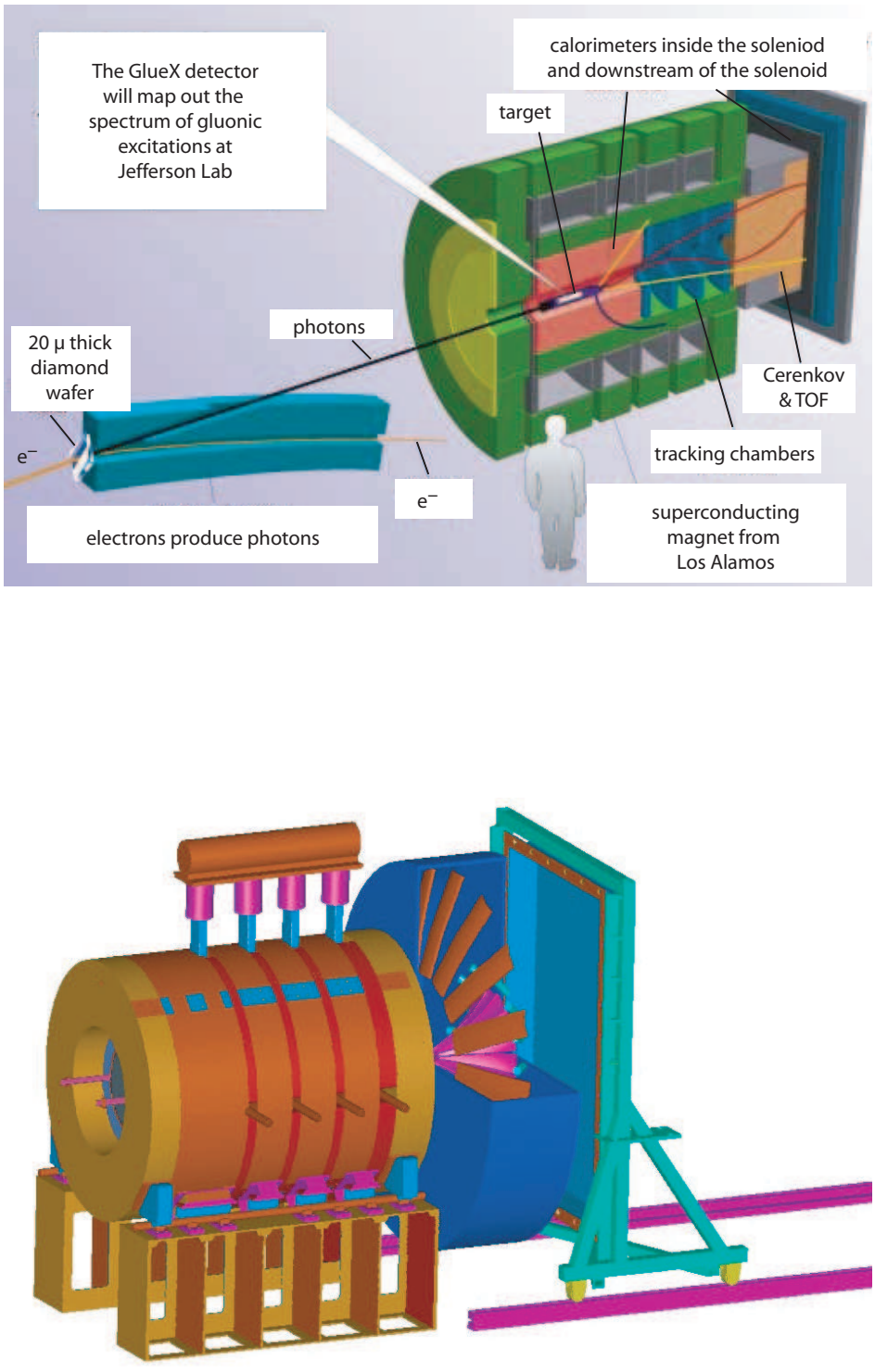

Figure 26: The proposed detector for the study of the photoproduction of mesons in the mass region around 2 GeV.